Journal of Geochemical Exploration 217 (2020) 106557

Contents lists available at ScienceDirect

Journal of Geochemical Exploration

journal homepage: www.elsevier.com/locate/gexplo

A regional soil and river sediment geochemical study in Baoshan area, Yunnan province, southwest China

Li Zhang[a,b,c,d], Jennifer McKinley[d], Mark Cooper[e], Min Peng[a,b,c], Qiaolin Wang[a,c], Yuntao Song[a,c], Hangxin Cheng[a,c,*]

[a] Key Laboratory of Geochemical Cycling of Carbon and Mercury in the Earth's Critical Zone, Institute of Geophysical & Geochemical Exploration, Chinese Academy of Geological Sciences, Langfang 065000, China
[b] China University of Geosciences, Beijing 100083, China
[c] Research Center of Geochemical Survey and Assessment on Land Quality, China Geological Survey, Langfang 065000, China
[d] School of Natural and Built Environment, Queen's University Belfast, Belfast BT7 1NN, UK
[e] Geological Survey of Northern Ireland, Belfast BT4 3SB, UK

ARTICLE INFO

Keywords:
NGSLQ
PTMs
CoDA
Principal component analysis
Enrichment factor
Baoshan

ABSTRACT

This study aims to better understand, at a regional scale, the concentration and distribution of selected chemical elements in surface environments and the influence of natural factors (geological background, geomorphology) and anthropogenic factors (mining activities, land-use, agricultural fertilization) on their distribution in the Baoshan area, Yunnan province, southwest China. Mineral resources (such as copper, lead, zinc, mercury, gold, silver) and carbonate and basalt parent materials in this area often lead to elevated potentially toxic metals (PTMs), which are widely distributed where mining activities have rapidly developed since last 20–30 years. This study makes use of 1574 surface soil data and 425 deep soil data from the National Geochemistry Survey of Land Quality project (NGSLQ), and 1585 archived river sediment data which were collected and analyzed for the Regional Geochemistry-National Reconnaissance program (RGNR). These data, once log-ratio (clr) transformed have been studied by compositional data analysis (CoDA), principle components analysis (PCA) and spatial analysis. In the Baoshan area, the concentration of elements As, B, (Br), Co, Cr, Cu, Hg, (I), Mn, (N), Ni, Sb, (Sc), (Se), V, Fe_2O_{3Total} and ($C_{Orgonic}$) are enriched compared to the China Soil Geochemical Baselines program (CGB) and RGNR data sets; while elements Sr and Na_2O are depleted compared to CGB and RGNR data sets. Influencing factors on surface soil, deep soil and river sediment composition of the study area are revealed. The distribution of most elements in surface soil, deep soil and river sediment are influenced by natural factors such that: Co, Cr, Cu, Ni, Sc, Ti, V, Fe_2O_{3Total} and MgO are controlled by the distribution of basic igneous rocks; Ca, Mg, Sr and pH are controlled by the distribution of carbonate rocks and basic igneous rocks; As, Hg, Sb, (Ag), Cd, Pb and Zn are controlled by mineralization; and other elements normally controlled by the distribution of clastic rocks and acid-intermediate rocks; while the organic matter such as Br, N, (P), S, $C_{Orgonic}$ and C_{Total} in soil data set are controlled by geomorphic (altitude and temperature). Anthropogenic factors are also recognized in the soil data set. For example: high pH values in paddy land and grassland, and low pH values in forested land, garden plot and dry cultivated land; in agricultural area fertilization has caused enrichment of the nutrient elements ($C_{Orgonic}$, C_{Total}, N, P, etc.,) in surface soil; while in areas of mining, surface soils are contaminated by PTMs (incl. Hg, As, Sb, Cu, Pb, Zn and Cd).

1. Introduction

1.1. Overview

Since 1999, the National Geochemistry Survey of Land Quality project (NGSLQ), has been carried out in agriculturally and industrially developed regions of China by the China Geological Survey (CGS). Prior to 2012 the NGSLQ was called the National Multi-Purpose Regional Geochemical Survey (NMPRGS). The purpose of the project is to provide modern, higher density, more sensitive, more systematic and

* Corresponding author at: Key Laboratory of Geochemical Cycling of Carbon and Mercury in the Earth's Critical Zone, Institute of Geophysical & Geochemical Exploration, Chinese Academy of Geological Sciences, Langfang 065000, China.
E-mail address: chenghangxin@igge.cn (H. Cheng).

https://doi.org/10.1016/j.gexplo.2020.106557
Received 6 November 2019; Received in revised form 3 April 2020; Accepted 24 April 2020
Available online 05 May 2020
0375-6742/

multi-medium geochemical data for supporting science-based decisions related to assessing land resources, protecting the surface environment, and improving the efficiency of agriculture (Li et al., 2014a). More than 200 million km^2 of land has been surveyed at a scale of 1:250000, mainly on the plains of eastern and central China and in some parts of southwest and northwest of China. A large volume of geochemical data of soil sample have been obtained, include total concentration of 54 elements and indictors (Ag, As, Au, B, Ba, Be, Bi, Br, Cd, Ce, Cl, Co, Cr, Cu, F, Ga, Ge, Hg, I, La, Li, Mn, Mo, N, Nb, Ni, P, Pb, Rb, S, Sb, Sc, Se, Sn, Sr, Th, Ti, Tl, U, V, W, Y, Zn, Zr, SiO_2, Al_2O_3, Fe_2O_{3Total}, MgO, CaO, Na_2O, K_2O, C_{Total}, $C_{Orgonic}$ and pH). Several atlases and papers have been published since this program was initiated, typically by the volume Exploring China: Environment and Resources published in the Journal of Geochemical Exploration in 2014 (Cheng et al., 2014a).

Soil and cultivatable land are the basis for food production and play an essential role in national food security. With competing pressures between population, resources and the environment, soil quality has become a major concern globally (Cicchella et al., 2008; Kelepertzis et al., 2013; Li et al., 2010; Li et al., 2014b; Luo et al., 2012; Zhang et al., 2013). The external morphology and internal characteristics of soil are determined by parent material, biology, climate, topography, time, and human activities (Dokuchaev, 1967; Jenny, 1941). The concentration and distribution of elements in soil are also controlled by those factors. The enrichment of chemical elements especially potentially toxic metals (PTMs) in soil by human activities (industrial and mining activities, agricultural fertilization and irrigation and urban living pollutants, etc.) have become recognized by public authorities and are well researched by scientists (Addo et al., 2012; Chiu et al., 2016; Hamzeh et al., 2011; Luo et al., 2012; McGrath and Tunney, 2010). While, the enrichment and deficit of elements in soil due to the geological background are mainly caused by the weathering process of parent materials. The critical role of the geological background in contributing to elevated chemical elements in soil is reviewed by a significant body of research in this field (e.g. Antibachi et al., 2012; Becquer et al., 2006; Bompoti et al., 2015; Bonifacio et al., 2010; Kelepertzis et al., 2013; Tashakor et al., 2014).

The geochemical mapping provides a more detailed information about the spatial variability of chemical components for environmental studies, particularly in discriminating potential sources of contribution (either anthropogenic and geogenic) in global, continent and regional scale (Albanese et al., 2007; Darnley and Garrett, 1990; Darnley et al., 1995; Gałuszka, 2007; Plant et al., 2001; Qu et al., 2017, 2019; Reimann and Caritat, 2005, 2017; Yuan et al., 2013; Sahoo et al., 2019a, 2019b, 2020; Salomão et al., 2019). The presences of mineral resources (such as copper, lead, zinc, mercury, gold, silver) and carbonate and basalt parent materials often lead to elevated PTMs in soil (Barsby et al., 2012; Cabral Pinto et al., 2017; Cheng, 2016; Cox et al., 2017; Goldhaber et al., 2009; Tolosana-Delgado and McKinley, 2016; Wang et al., 2015; Zhang et al., 2002). This can be seen in soils in the Baoshan area, Yunnan province, southwest China, where mining activities have developed rapidly in the past two to three decades. The Baoshan area (6220 km^2) was surveyed in 2016 at a scale of 1: 250000 to better understand the regional geochemical status and the influence of natural factors (geological background, geomorphology), and anthropogenic activities (mining activities, land-use, agricultural fertilization) on the distribution of selected elements in surface environments. A total of 1585 archived river sediment samples, which were collected and analyzed as part of the Regional Geochemistry-National Reconnaissance program (RGNR) in China, have been used as the dataset for this study, and it has not been published elsewhere.

Geochemical data do not change independently and freely, but must accommodate each other within the constant sum constraint of the closed composition, which was identified to induce spurious behavior on the correlation coefficient (Chayes, 1960), called negative bias (the negative correlation coefficients between major components) and the spurious correlation effect (the correlation between two components unpredictably changes when considering different sub-compositions) (Tolosana-Delgado and McKinley, 2016). Aitchison (1981, 1982, 1986) and Egozcue et al. (2003) proposed log-ratio transformations, in the form of the pairwise log-ratio transformation (pwlr), the additive log-ratio transformation (alr) and the centred log-ratio transformation (clr), and isometric log-ratio (ilr) transformation to make the classical (Euclidean) statistical methods applicable to compositional data. The field of compositional data analysis (CoDA) has been widely developed since Aitchison's work to solve the limitations on geochemical data (e.g. Boogaart and Tolosana-Delgado, 2013; Egozcue et al., 2003; Pawlowsky-Glahn and Buccianti, 2011; Pawlowsky-Glahn and Egozcue, 2001). There are a series of mathematical tools for extracting meaningful results from compositional data, yet none of these transformation methods is inherently better than the other. McKinley et al. (2016) proposed two approaches (a) knowledge-driven log-ratios, chosen to highlight certain geochemical relations or to filter known artefacts (e.g. dilution with SiO_2 or volatiles); (b) log-contrasts, that employ suitable statistical methods (such as classification techniques, regression analysis, principal component analysis, and clustering of variables) with log-ratio transformed data to extract potentially interesting geochemical summaries to solve the limitations on geochemical data.

This study uses CoDA methods and focuses on 1) the concentration and distribution of selected chemical elements at a regional scale in soil and river sediments of the Baoshan area; 2) the influence of natural factors (geological background, geomorphology) and anthropogenic factors (mining activities, land-use, agricultural fertilization) on the pattern of chemical concentrations in soil and river sediments; 3) the main controlling factors on the occurrence of PTMs (As, Cd, Cr, Cu, Hg, Ni, Pb, Zn, etc.).

1.2. Study area

Baoshan is located in the western Yunnan province with complex topography, at low latitude and with moderate elevation. Baoshan has a mild subtropical highland climate, with short, mild, dry winters, and warm, rainy summers. Contour maps of altitude, and average surface soil temperature and rainfall are shown in Fig. 1. Variation of average temperature is directly related to altitude. Rainfall is greatest in the western and southern parts of the study area. The main types of land-use in the study area are: forest land, dry cultivated land, paddy land, grassland, garden plot, with few water areas and other types (including: residential quarter and industrial and mining land, and unused land). The simplified land-use map is shown in Fig. 2a.

Geologically, the study area is located in the Sanjiang area of Yunnan province, which consists of Tengchong, Baoshan, and Lanping-Simao blocks (Fig. 2b, c; Dong et al., 2013; Li et al., 2015; Wang et al., 2010). The rock types of the Baoshan Block mainly consist of Paleozoic to Mesozoic sedimentary rocks, and Early Paleozoic and Late Mesozoic-Early Cenozoic magmatic rocks (Dong et al., 2013; Wang et al., 2013). Exposed within the study area are mainly Quaternary to Precambrian stratum and sparse granite and diabase intrusions. Basalt occurs in the Carboniferous and Jurassic rock sequences that are mainly distributed in the western and northeast part of the study area. The major rock types of the all strata in each geological age are shown in Fig. 2d. Mineral deposits, which are often associated with PTMs pollution in soil, are widely distributed across the study area and include copper-lead-zinc and mercury workings (Fig. 2d).

2. Methodology

2.1. Sample collection and preparation

This study uses soil samples collected in 2016 as part of the NGSLQ project, and supplemented archived river sediment samples collected during the RGNR program. A systematic, regular grid sampling design was applied for both the NGSLQ and RGNR (CGS, 2005, 2014; Xie et al.,

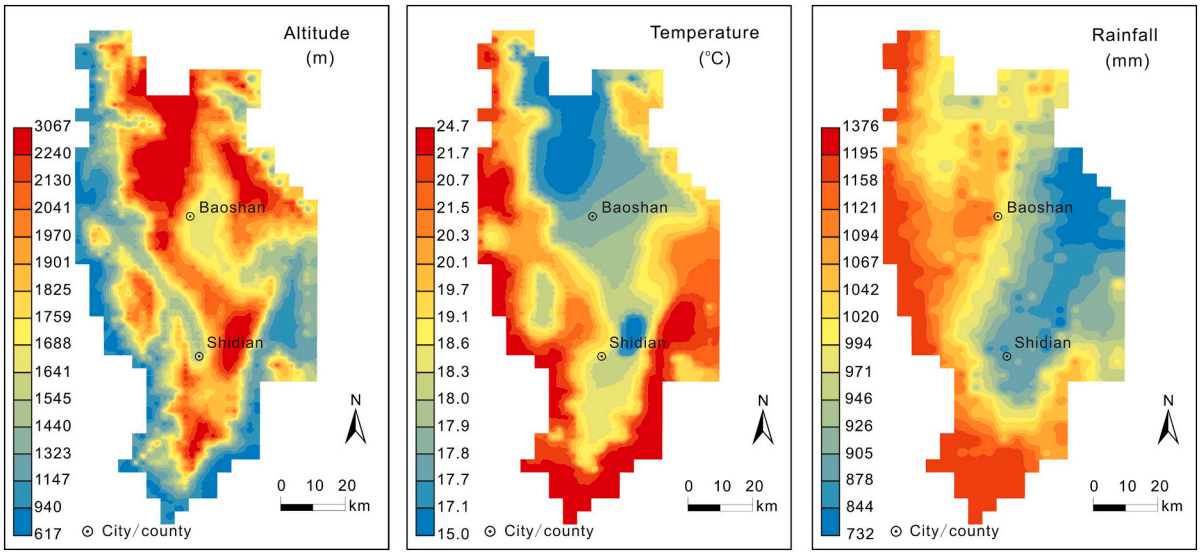

Fig. 1. Contour maps of altitude, average surface soil (0 cm) temperature, and annual rainfall for study area.

2008; Xie and Cheng, 2014).

Surface soil at 0–20 cm depth were collected at a density of 1 sample/km^2 with one main sample and 3–5 sub-holes within 50 m of the sampling site. Deep soil at 150–180 cm depth, or soil from C horizon if soil depth is <150 cm, were taken at a density of 1 sample/4 km^2 in the study area. Among surface soil and deep soil samples, about 2%–3% of the sampling sites were re-sampled to assess sampling variation. Each sample site was selected from the most representative land-use types within the most common soil types in the sampling cell. In order to reduce the analytical cost, samples from 4 km^2 for surface soil and 16 km^2 for deep soil were composited (Fig. S2, Supplementary file). The sample collection and preparation details are provided by Li et al. (2014a) and Supplementary file. The soil samples were disaggregated using a wooden hammer during air-drying and sieved with −20 mesh screen (<0.84 mm), once dried they were further processed to −200 mesh (<0.074 mm) for analysis.

Detailed sampling methods and prepare processes for river sediments are described in previous papers (Xie et al., 2008; Xie and Cheng, 2014). Briefly, river sediment samples were collected at an average density of 1 sample km^2 from first-order streams, and all samples within a 4 km^2 grid were composited to obtain a sample for chemical analysis. The river sediment samples were sampled with −60 mesh (<0.42 mm) in the field and were further processed to −200 mesh (<0.074 mm) for analysis.

All the sampling positions were pinpointed by Global Positioning System (GPS). The central locations of composited surface soil, deep soil and river sediments are showed in Fig. S2 (Supplementary file), include a total of 1574 surface soil data, 425 deep soil data, and 1585 river sediment data.

2.2. Chemical analysis and quality control

The total content of 54 elements and indictors (Ag, As, Au, B, Ba, Be, Bi, Br, Cd, Ce, Cl, Co, Cr, Cu, F, Ga, Ge, Hg, I, La, Li, Mn, Mo, N, Nb, Ni, P, Pb, Rb, S, Sb, Sc, Se, Sn, Sr, Th, Ti, Tl, U, V, W, Y, Zn, Zr, SiO_2, Al_2O_3, Fe_2O_{3Total}, MgO, CaO, Na_2O, K_2O, C_{Total}, $C_{Orgonic}$ and pH) of all soil samples were determined in the Central Analytical Laboratory of the Institute of Geophysical & Geochemical Exploration (IGGE). The analytical methods and detection limits are listed in Table S1 (Supplementary file). The detailed analytical procedures are reviewed by Zheng et al. (2005).

Internal and external controls were implemented during the routine analysis to check accuracy and precision. Briefly, certified reference materials (CRMs) and blind reference materials (BRMs) were analyzed with samples simultaneously to assess the accuracy and precision of sample analysis. The detailed description can be seen in Li et al. (2014a) and Supplementary file. The requirements of accuracy and precision were listed in Tables S2 and S3 (Supplementary file), while for pH, the relative deviation (RD) between sample and CRMs should be satisfied with $|\Delta pH| \leq 0.1$. The accuracies and precisions of all elements in all samples are satisfied with the analytical requirements developed in the NMPRGS/NGSLQ project (CGS, 2005, 2014).

2.3. Statistical analysis and mapping

Centred log-ratio transformation methods have been used in this study using CoDAPack, which is a freeware package that implements most of the basic statistical methods suitable for compositional data (Thio-Henestrosa and Martin-Fernandez, 2006).

ArcMap™ was used for spatial analysis of all the data. SPSS 21.0 software was used for statistical analysis, principal component analysis (PCA) on the clr transformed data. All geochemical maps are plotted by inverse distance weighted (IDW). The colour ramp for all geochemical maps used ten division quantile colour ramp. The PCA was performed using the correlation matrix after quartic max rotation and attention was given to the elements with loadings higher than 0.5 or lower than −0.5.

3. Results and discussion

Tables 1 and 2 provide a summary of the soil and river sediment geochemical data used in this study with a comparison to continental-scale data sets from China. The China soil data set is comprised of topsoil samples (0–25 cm) and subsoil samples (>100 cm) collected from 3382 drainage catchments in China by the China soil Geochemical Baselines program (CGB; Wang et al., 2016). The China river sediment data set is comprised of all the samples collected since 1978 in the RGNR program, the median of the data set, after eliminating outliers from a data population with X ± 3S as the critical value, is used as an estimate value of geochemical background values (Shi et al., 2016).

Several elements stand out in the Baoshan data set: As, B, Ce, Co, Cr, Cu, F, Ga, Ge, Hg, I, La, Mn, N, Nb, Ni, Rb, Sb, Sn, Th, Ti, Tl, V, Y, Zn, Al_2O_3, Fe_2O_{3Total}, and $C_{Orgonic}$ are higher than 85% of CGB data which indicates that the element content is significantly higher than the typical value in China, which is called a positive anomaly (Wang et al., 2016). Furthermore, of those elements, the concentrations of As, B, Co,

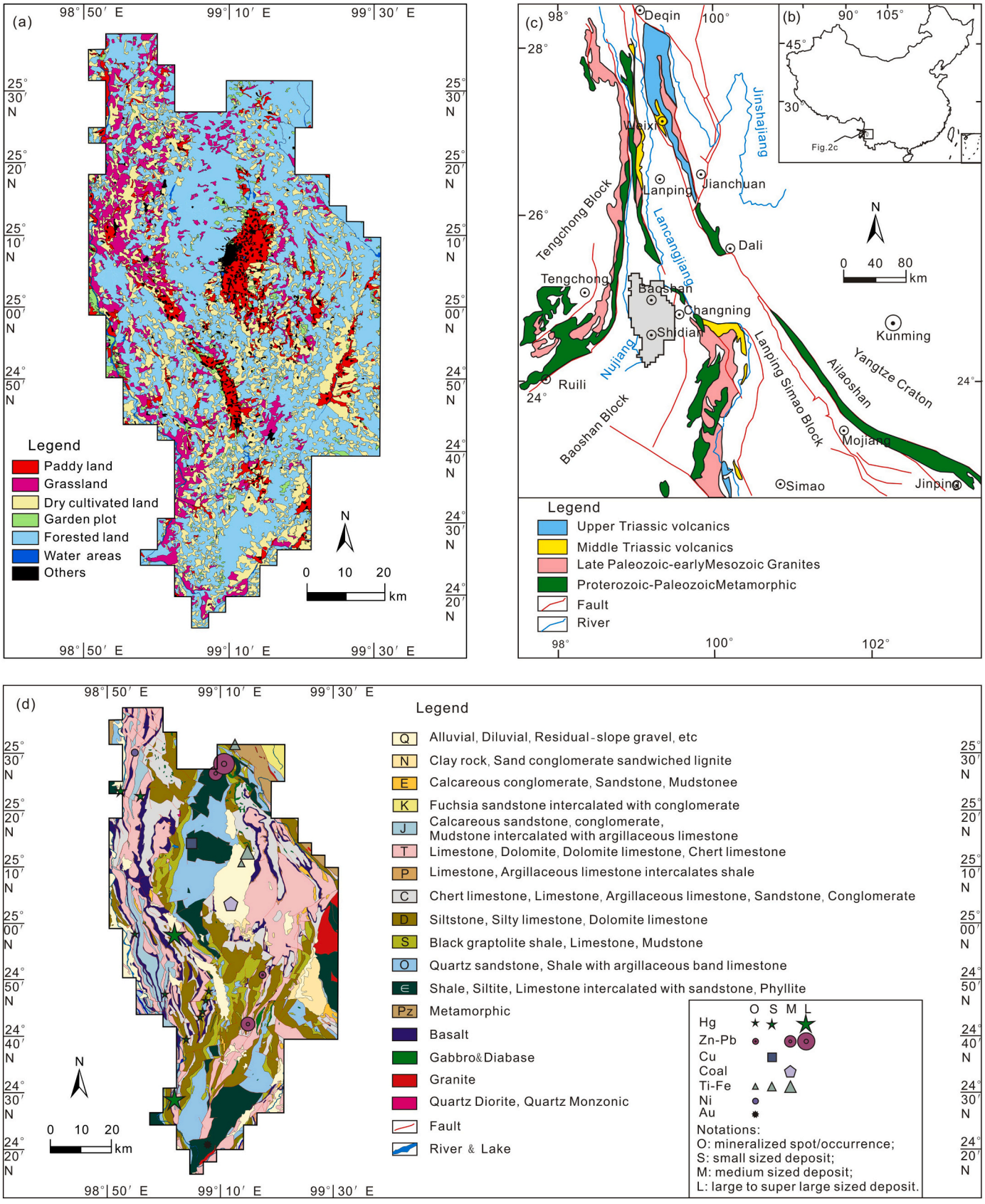

Fig. 2. General situation of study area. (a) Simplified land-use map of study area. (b, c) Simplified tectonic map of Yunnan Sanjiang area. (d) Simplified geological and mineral deposits map of study area (geological map simplified from Yunnan geological and mineral development bureau regional geological survey team, 1981, 1983, 1986; mineralization map from CGS mineral resources database http://geocloud.cgs.gov.cn).

Table 1
Statistical comparison of Baoshan soil data set with China Soil Geochemical Baselines (CGB) data set.

Elements	Depths	This study				CGB data (Wang et al., 2016)			
		Median	Mean	Min	Max	LBGB	BGB	HBGB	AGB
						25%	50%	75%	85%
Ag (ng/g)	Surface	84	103	27	4203	59	77	102	121
	Deep	78	93	32	2133	55	70	90	107
As(μg/g)	Surface	16.4	23.0	0.5	909.1	6	9	14	17
	Deep	18.7	26.7	1.8	536.8	6	9	13	17
Au (ng/g)	Surface	1.76	2.71	0.15	285.20	0.8	1.3	2	2.6
	Deep	2.03	2.43	0.53	25.47	0.7	1.1	1.8	2.3
B (μg/g)	Surface	79	82	8	513	30	43	61	75
	Deep	78	81	20	232	26	41	59	71
Ba (μg/g)	Surface	327	381	105	9035	427	512	610	665
	Deep	342	390	90	1556	431	522	628	689
Be (μg/g)	Surface	2.45	2.53	0.90	13.58	1.7	2	2.4	2.7
	Deep	2.70	2.80	1.33	9.42	1.6	2	2.5	2.8
Bi (μg/g)	Surface	0.43	0.49	0.03	7.12	0.21	0.3	0.4	0.51
	Deep	0.45	0.49	0.17	6.47	0.19	0.27	0.37	0.46
Br (μg/g)	Surface	4.58	6.12	1.19	66.84	1.5	2.2	3.5	4.5
	Deep	3.48	4.45	0.50	24.94	1.5	1.8	2.8	3.6
Cd (ng/g)	Surface	187	269	15	5352	96	137	197	261
	Deep	131	200	15	3215	79	110	159	205
Ce (μg/g)	Surface	90.7	90.6	27.6	237.3	50	64	77	86
	Deep	93.8	94.5	38.4	226.1	46	62	77	86
Cl (μg/g)	Surface	38	45	10	841	55	78	171	538
	Deep	39	45	25	370	48	72	164	425
Co (μg/g)	Surface	22.02	24.15	2.93	72.31	8	11	14	16
	Deep	23.97	25.10	4.72	64.14	7	11	14	16
Cr (μg/g)	Surface	113	128	10	422	37	53	68	79
	Deep	119	130	35	299	33	50	68	79
Cu (μg/g)	Surface	40.7	48.7	3.1	652.2	14	20	27	33
	Deep	45.2	49.5	7.1	277.4	13	19	26	31
F (μg/g)	Surface	665	749	146	2219	372	488	591	657
	Deep	700	792	289	2159	343	456	575	648
Ga (μg/g)	Surface	21.2	21.2	10.1	32.9	12	15	18	19
	Deep	22.6	22.7	13.9	35.4	12	15	18	19
Ge (μg/g)	Surface	1.64	1.67	0.70	4.39	1.1	1.3	1.5	1.6
	Deep	1.75	1.78	0.35	5.16	1.1	1.3	1.5	1.6
Hg (ng/g)	Surface	105	178	4	6813	13	26	56	87
	Deep	112	135	19	2353	11	18	36	55
I (μg/g)	Surface	4.95	5.52	0.39	29.01	0.7	1.1	1.8	2.3
	Deep	4.76	5.13	0.66	17.91	0.6	1	1.7	2.4
La (μg/g)	Surface	47.5	47.7	13.6	112.5	25	33	40	44
	Deep	47.5	48.9	21.4	139.3	23	32	39	44
Li (μg/g)	Surface	37.5	38.7	9.3	221.2	23	30	38	43
	Deep	37.4	37.9	11.8	91.1	21	29	37	43
Mn (μg/g)	Surface	997	1110	88	9721	425	569	725	825
	Deep	962	1053	89	3020	423	562	728	842
Mo (μg/g)	Surface	1.03	1.17	0.15	14.76	0.5	0.7	1.1	1.4
	Deep	1.05	1.19	0.33	4.86	0.5	0.7	1	1.3
N (μg/g)	Surface	1700	1903	315	7396	343	707	1169	1540
	Deep	824	900	315	2265	217	399	683	888
Nb (μg/g)	Surface	20.40	21.02	9.20	70.30	10	13	16	18
	Deep	20.19	20.90	11.41	56.10	9	12	16	19
Ni (μg/g)	Surface	51.1	57.9	3.7	361.1	16	24	31	36
	Deep	57.7	61.0	18.8	175.9	15	22	31	36
P (μg/g)	Surface	820	891	321	3424	411	570	748	869
	Deep	537	592	219	1707	341	488	635	724
Pb (μg/g)	Surface	33.7	45.2	4.4	2106.4	18	22	28	34
	Deep	30.7	46.0	10.0	3323.3	16	21	26	32
Rb (μg/g)	Surface	131.5	128.9	19.6	345.3	80	96	115	130
	Deep	137.2	135.7	41.9	276.9	78	96	117	134
S (μg/g)	Surface	272	303	15	2894	156	245	430	757
	Deep	127	144	53	772	97	166	329	578
Sb (μg/g)	Surface	1.80	3.56	0.03	145.46	0.47	0.73	1.08	1.38
	Deep	1.70	3.03	0.24	32.35	0.43	0.67	1.03	1.31
Sc (μg/g)	Surface	17.1	18.7	4.1	48.7	7	10	12	13
	Deep	18.8	20.1	7.5	43.7	7	9	12	13
Se (μg/g)	Surface	0.33	0.35	0.03	1.47	0.11	0.17	0.27	0.35
	Deep	0.29	0.30	0.05	1.17	0.08	0.13	0.21	0.27
Sn (μg/g)	Surface	4.07	4.36	1.19	89.64	2	3	4	5
	Deep	4.04	4.20	1.80	21.21	2	3	3	4
Sr (μg/g)	Surface	62	75	17	415	117	197	261	301
	Deep	63	73	16	323	116	197	264	310

(*continued on next page*)

Table 1 (*continued*)

Elements	Depths	This study				CGB data (Wang et al., 2016)			
		Median	Mean	Min	Max	LBGB	BGB	HBGB	AGB
						25%	50%	75%	85%
Th (μg/g)	Surface	16.17	16.37	2.90	59.26	8	11	13	15
	Deep	15.69	16.17	6.76	56.99	8	10	13	15
Ti (μg/g)	Surface	6087	6464	2641	15,932	2763	3498	4171	4611
	Deep	5943	6353	3050	18,382	2582	3406	4191	4662
Tl (μg/g)	Surface	0.84	0.90	0.15	6.56	0.5	0.6	0.7	0.8
	Deep	0.86	0.94	0.29	5.91	0.5	0.6	0.8	0.9
U (μg/g)	Surface	3.01	3.19	0.39	14.11	2	2.5	3.2	3.8
	Deep	3.08	3.26	1.21	13.58	1.8	2.4	3.1	3.7
V (μg/g)	Surface	134.7	147.4	32.3	343.2	51	70	88	100
	Deep	141.9	153.4	64.6	318.0	48	67	88	100
W (μg/g)	Surface	2.0	2.5	0.4	123.2	1.2	1.6	2	2.5
	Deep	2.1	2.6	0.8	32.6	1.1	1.5	2	2.5
Y (μg/g)	Surface	32.9	34.5	14.1	93.0	19	24	28	30
	Deep	33.5	35.9	15.4	126.1	18	23	27	30
Zn (μg/g)	Surface	100.4	114.8	28.0	1943.0	48	66	84	95
	Deep	100.2	115.5	34.6	1073.4	43	60	79	99
Zr (μg/g)	Surface	246	248	95	594	170	230	288	321
	Deep	232	236	119	428	157	215	279	315
SiO_2 (wt%)	Surface	61.1	61.0	37.2	84.2	61.2	66.7	72	75.1
	Deep	59.7	59.5	42.8	80.9	62.5	67.9	72.9	75.7
Al_2O_3 (wt%)	Surface	16.5	16.6	8.3	26.1	10.3	11.9	13.3	14.1
	Deep	18.3	18.3	11.0	26.0	10.1	11.9	13.4	14.2
Fe_2O_{3Total} (wt%)	Surface	7.33	7.76	1.97	16.29	3.2	4.2	5.3	5.9
	Deep	8.05	8.34	3.38	15.55	3	4.1	5.2	5.8
MgO (wt%)	Surface	1.11	1.44	0.26	11.22	0.9	1.43	2.2	2.65
	Deep	1.28	1.56	0.38	9.21	0.86	1.36	2.05	2.47
CaO (wt%)	Surface	0.76	1.60	0.10	18.30	1.12	2.74	6.08	7.79
	Deep	0.62	1.66	0.08	15.87	1.02	2.57	5.87	7.61
Na_2O (wt%)	Surface	0.15	0.27	0.05	3.25	1.06	1.75	2.29	2.64
	Deep	0.17	0.31	0.05	2.13	1.05	1.81	2.38	2.76
K_2O (wt%)	Surface	2.35	2.34	0.59	6.29	2.03	2.36	2.74	2.97
	Deep	2.56	2.54	0.69	4.80	2.03	2.36	2.79	3.06
$C_{Orgonic}$ (wt%)	Surface	1.53	1.74	0.36	7.94	0.3	0.6	1.1	1.5
	Deep	0.59	0.68	0.05	3.19	0.2	0.3	0.5	0.8
C_{Total} (wt%)	Surface	1.82	2.12	0.31	11.33	0.8	1.3	2	2.5
	Deep	0.74	0.96	0.21	6.02	0.4	0.9	1.7	2.1
pH	Surface	6.46	6.45	4.13	8.33	7	8	8.3	8.4
	Deep	6.57	6.56	4.32	8.34	7.4	8.1	8.4	8.5

LBGB: low background geochemical baseline; BGB: background geochemical baseline; HBGB: high background geochemical baseline; AGB: abnormal geochemical baseline; wt%: weight percent.

Cr, Cu, Hg, I, Mn, N, Ni, Sb, Sc, Se, V, Fe_2O_{3Total} and $C_{Orgonic}$ are enriched by approximately a factor of two or more compared to the China data; While Ba, Cl, Sr, SiO_2, CaO and Na_2O are lower than 25% of CGB data which indicates that the element content is significantly depleted relative to the typical value, which is called a negative anomaly (Wang et al., 2016). Among those elements, Sr, CaO and Na_2O are depleted by a factor of two to ten compared to the CGB data. By comparison, elements in the river sediment dataset enriched by approximately a factor of two or more in Baoshan area compared to the whole RGNR data set, include As, B, CaO, Cd, Co, Cr, Cu, Hg, Mn, Ni, Sb, V and Fe_2O_{3Total}, while Sr and Na_2O are depleted.

The following rock groupings were made in order to simplify the spatial distribution of similar rock types across the region: conglomerate, sandstone, siltstone, mudstone, shale and some undivided sediment stratum are combined as Clastic rocks; limestone, dolomite, argillaceous limestone, argillaceous dolomite, calcite dolomite, dolomite limestone, siliceous limestone and chert limestone are combined as Carbonate rocks; basalt, olivine basalt, gabbro and diabase are combined as Basic igneous rocks; muscovite granite, granitoid and dacite are combined as Acid-Intermediate rocks; Quaternary stratum are combined as Quaternary; metamorphic rocks (no matter what their origin are) are combined as Metamorphic rocks; finally some unknown rock types are combined as Unknown. Numbers of samples associated with these combined rock groupings and relationship with mineralization are shown in Table S4 (Supplementary file).

3.1. Spatial patterns of major elements in soil and river sediments

The geochemical results of major elements for soil and river sediment show distinct spatial patterns in study area as shown by the box plots (Fig. 3) and the plan geochemical maps (Fig. 4).

It is apparent from Fig. 3 that Mg in surface soil, deep soil and river sediment (MgO median: 2.11 wt% in surface soil, 1.97 wt% in deep soil, 3.65 wt% in river sediments) is strongly associated with basic igneous rocks, especially basalt rocks of Carboniferous and Jurassic age distributed in the western and northeast part of the study area (Fig. 4). Similar characteristics can be seen in Fe (Fe_2O_{3Total} median: 10.60 wt% in surface soil, 9.74 wt% in deep soil, 9.70 wt% in river sediments), and Ca (CaO median: 2.11 wt% in surface soil, 1.37 wt% in deep soil, 5.25 wt% in river sediments), their distribution patterns are related to basic igneous rocks and basalt rocks as well (Fig. 3).

Elements Si and K show similar distribution in soil and river sediment to one another (Fig. 4), the highest concentrations distributed in the central and southeastern parts of study area. The highest median value of K in surface soil (K_2O median: 3.94 wt%), deep soil (K_2O median: 3.3 wt%) and river sediments (K_2O median: 3.60 wt%) are from samples taken from acid-intermediate rock parent material (Fig. 3). The majority of high K are, however, related to samples taken

Table 2
Statistical comparison of Baoshan river sediment data set with Regional Geochemistry-National Reconnaissance (RGNR) data set.

Elements	This study				China data (Shi et al., 2016)	SW China data (Shi et al., 2016)
	Median	Mean	Min	Max	Median	Median
Ag (ng/g)	73	102	20	5204	69	110
As (μg/g)	15.2	21.5	0.7	615.6	8	9.9
Au (ng/g)	1.1	1.69	0.1	70	1.1	2.1
B (μg/g)	60	63	8	423	41	52
Ba (μg/g)	333	382	80	2986	474	575
Be (μg/g)	2.1	2.16	0.1	8.5	2	2.2
Bi (μg/g)	0.3	0.4	0.03	12.8	0.3	0.42
Cd (ng/g)	200	395	10	56,700	110	140
Co (μg/g)	24.1	26	5.7	69.5	11	11
Cr (μg/g)	98	114	9	607	54	74
Cu (μg/g)	39	49	2	1735	20	26
F (μg/g)	586	664	170	2170	460	495
Hg (ng/g)	84	237	9	126,600	27	122
La (μg/g)	41	42	9	131	36	42
Li (μg/g)	32	32	7	100	30	35
Mn (μg/g)	1062	1136	134	3758	622	640
Mo (μg/g)	0.8	0.9	0.1	15	0.7	0.9
Nb (μg/g)	17	18	3	136	15	17
Ni (μg/g)	49	55	5	814	22	29
P (μg/g)	561	630	182	7636	535	610
Pb (μg/g)	27	95	5	39,300	22	31
Sb (μg/g)	1.6	3.21	0.1	77.7	0.6	1.35
Sn (μg/g)	3.2	3.64	0.1	60	2.7	4.4
Sr (μg/g)	68	80	4	696	129	165
Th (μg/g)	11.3	12	2.9	157.2	11	13
Ti (μg/g)	5444	5872	362	31,613	3881	4450
U (μg/g)	2.4	2.607	0.5	23.9	2.2	2.2
V (μg/g)	125	137	34	434	75	88
W (μg/g)	1.9	2.1	0.2	45	1.6	2.4
Y (μg/g)	27	29	10	224	24	28
Zn (μg/g)	86	108	6	4747	65	80
Zr (μg/g)	236	249	48	1776	248	275
Al_2O_3 (wt%)	14.2	14.25	4.2	26.4	12.8	12.8
CaO (wt%)	2	3.58	0.03	28.9	1.3	3.5
Fe_2O_{3Total} (wt%)	6.8	7.2	0.1	17.2	4.3	4.7
K_2O (wt%)	1.9	2.03	0.3	6.3	2.4	2.3
MgO (wt%)	1.2	2.16	0.3	16.2	1.2	1.7
Na_2O (wt%)	0.3	0.38	0.05	3.7	1.3	1.5
SiO_2 (wt%)	58.7	58.91	16	90.9	65.5	63.9

wt%: weight percent.

from clastic rock parent material (K_2O median: 2.49 wt% in surface soil, 2.84 wt% in deep soil, and 2.3 wt% in river sediments, respectively) and metamorphic rock parent material (2.96 wt% in surface soil, 2.78 wt% in deep soil, and 2.9 wt% in river sediments, respectively). The element Si behaves similarly to K, with high median values related to samples from clastic rock and metamorphic rock parent material. The elements Na and Al show highest median values in samples taken from acid-intermediate rock parent material, and little variation among samples sourced from other rock type parent material (Fig. 3).

Organic carbon is relatively higher in samples taken from surface soil taken from Quaternary parent material ($C_{Organic}$ median: 1.74 wt% in surface soil), relative to samples taken from acid-intermediate rock parent material ($C_{Organic}$ median: 0.97 wt% in surface soil) (Fig. 3). Though not shown by the figures here, it is worth noting that C_{Total}, N, P, Br, and S show similar characteristic to $C_{Organic}$, and can be explained by agricultural fertilization in areas with Quaternary parent material. It is also clear from Fig. 4, that there is an observable relationship between $C_{Organic}$ with altitude and temperature such that at lower temperatures and higher altitudes carbon turnover is reduced, which results in increased carbon accumulation even under conditions of lower productivity and carbon input.

In summary, high Fe, Mg, and Ca concentrations in soil and river sediments are distributed in western and northeastern parts of the study area, and are related to basalts with Carboniferous and Jurassic ages. High Si and K are distributed in the central and southeastern parts of study area, and are related to acid-intermediate rock parent material, Cambrian- and Ordovician-aged clastic rocks and Precambrian metamorphic rocks. The highest Na and Al concentration are related to samples from acid-intermediate rock parent material. Total carbon and $C_{Organic}$ in soils are mainly related to altitude and temperature, however, agricultural fertilization in Quaternary areas has caused its enrichment in surface soils (Fig. 4).

3.2. Spatial patterns of trace elements in soil and river sediments

The box plots presented for trace elements typically associated with basic igneous rocks (Cr, Co, Ni, Mn, Cu, V and Sc (not showed); Fig. 5), acid-intermediate rocks (La, Sr, Li, Ce (not showed) and Rb (not showed); Fig. 5) or mineralization-style typical in the study area (Pb, Zn, Cd, As, Sb and Hg; Fig. 6).

Chromium, Co and Ni are enriched in basic igneous rocks, and therefore exhibit obviously high values in overlying soil and nearby river sediments. The highest median values for Cr (183.96 μg/g in surface soil, 161.14 μg/g in deep soil, and 182.75 μg/g in river sediments), Ni (77.88 μg/g in surface soil, 72.17 μg/g in deep soil, and 75.85 μg/g in river sediments) and Co (38.26 μg/g in surface soil, 34.04 μg/g in deep soil, and 37.55 μg/g in river sediments) occur in those samples comprised of mostly basic igneous rock parent material (Fig. 5). Similar distribution characteristics are also observed with Fe and Mg. The highest concentrations of Cr, Co and Ni mainly occurred in the western and northeastern parts of the study area (Fig. 7), where Carboniferous and Jurassic basalt rocks are present. Cobalt, Ni, Mn, Cu, V and Sc (not showed) show similar patterns to Cr.

Lanthanum, Sr, Li, Ce, and Rb are typically higher in samples taken from acid-intermediate rock parent material than in samples from basic rock parent material. The content of La is conspicuously higher in soil and river sediments related to acid-intermediate rocks (median value: 72.87 μg/g in surface soil, 89.15 μg/g in deep soil, and 65.5 μg/g in river sediments, respectively), and similar with Sr (median value: 108.30 μg/g in surface soil, 93.43 μg/g in deep soil, and 123.50 μg/g in river sediments, respectively) (Fig. 5). High concentrations of La are distributed in all parts of the study area with basic igneous rocks, carbonate rocks and Precambrian metamorphic rocks (Fig. 7). Cerium, Rb and Li are not shown but have similar patterns to La. Furthermore, similar to K, high Rb (not shown) concentrations show a similar distribution to Cambrian- and Ordovician-aged clastic rocks and Precambrian metamorphic rocks in the study area. This may relate to the substitution of Rb for K in potassium-feldspars. Similar to the distribution of Ca, high Sr (not showed) concentrations are related to carbonate rocks and basic igneous rocks. This is probably related to Sr being known to substitute for Ca in minerals such as feldspars and carbonates.

Lead concentration is elevated in those samples taken adjacent to zinc-lead and copper mineralization (Fig. 6), that is mainly distributed in the middle north and middle south of the study area (Fig. 7). Zinc and Cd are not shown but show similar distributions to Pb. The highest Hg, As (not showed) and Sb (not showed) concentrations occur in samples adjacent to mercury mineralization. Samples with high concentrations of Hg, As and Sb also occur adjacent copper-lead-zinc deposits (Fig. 7). In the box plots (Fig. 6) the concentrations of Hg, As and Sb are similar between samples taken adjacent the mercury deposit and samples taken adjacent to other types of mineralization.

3.3. Natural impacts on elements distribution in soil and river sediments

Except for $C_{Organic}$ and related organic matter related elements in surface soil in Quaternary area talked above, the distribution patterns of element described above reflects the interaction of geological

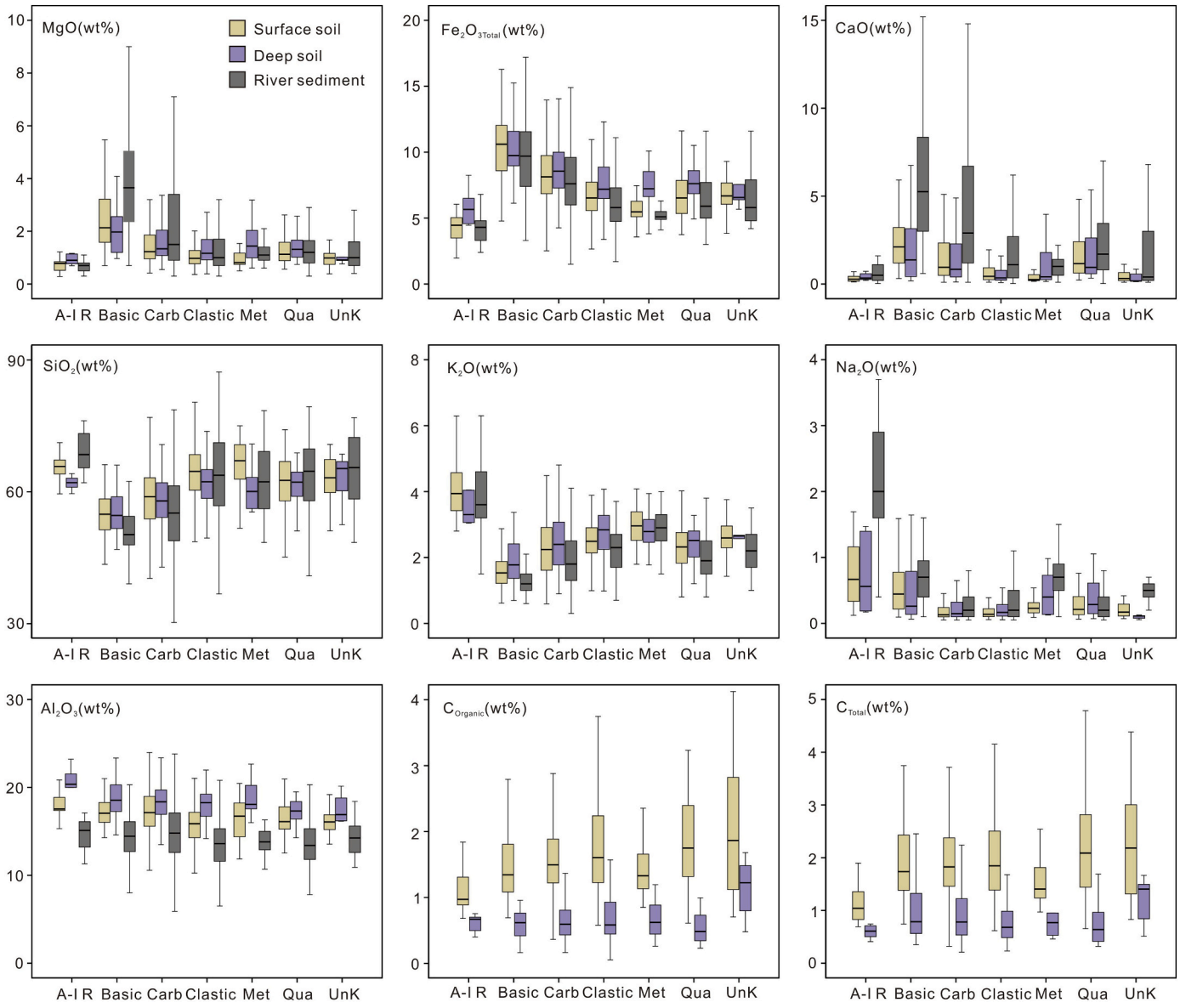

Fig. 3. Box plots of major elements of surface soil, deep soil and river sediments according to rock type groupings.

background (parent materials and mineralization) and geomorphology. To find the geochemical associations and spatial distribution between the elements in soil and river sediments, and to simplify the variables to find the main controlling factors of the distribution of elements in the study area, the correlation matrix based on PCA was performed with the clr data.

3.3.1. Surface soil

Five PCs accounting for 63.9% of the total variance were identified using a scree plot. The results of each PC and the PC geochemical maps are shown in Fig. 8, where the geological, mineralization, altitude contour and land-use maps are also presented to help the comparison. The low proportion of the variance for each PC reflects the complexity of soil composition in the Baoshan area. The following observations were made:

PC1: clr. Co (−0.82), clr. Cr (−0.89), clr. Cu (−0.83), clr. Ni (−0.81), clr. Sc (−0.85), clr. Ti (−0.70), clr. V (−0.88), clr. Fe_2O_{3Total} (−0.86), clr. MgO (−0.61) are associated with high negative loadings. The distribution of these siderophile elements in soil clearly shows the influence of basic igneous rock (especially basaltic rock) parent material, and the presence of typical mafic minerals including pyroxene (Mg, Fe, Ca, V, Ti, Cr, Sc), olivine (Fe, Mg, Ni), amphibole (Fe, Mg), chromite (Fe, Mg, Cr), titanite (Ti, Fe), and serpentine (Co, Cr, Ni; Cabral Pinto et al., 2017). Conversely, lithophile elements are associated with high positive loadings: clr. B (0.71), clr. Ba (0.51), clr. Be (0.51), clr. Bi (0.57), clr. Ce (0.71), clr. F (0.55), clr. La (0.69), clr. Rb (0.88), clr. Sn (0.63), clr. Th (0.79), clr. Tl (0.73), clr. U (0.54), clr. K_2O (0.77). The distributions of these elements are associates with soils sourced from clastic rock parent material in the middle of study area, and acid-intermediate rock parent material in the east of the study area.

PC2: clr. Br (−0.53), clr. N (−0.90), clr. P (−0.70), clr.S (−0.82), clr. $C_{Organic}$ (−0.91), clr. C_{Total} (−0.88) have high negative loadings, related to soils located in the higher altitude middle and northeastern parts of the study area. Lower temperature in these higher altitude areas limits organic matter turnover, which results in their increased accumulation even under conditions of lower productivity of organic related elements input. This is comparable to findings in other studies in southeast Germany (Bavaria) and Switzerland looking at organic carbon storage (Leifeld et al., 2005; Wiesmeier et al., 2013). While, this PC is also in a minor related to the agricultural fertilization in Quaternary areas show little reflect the as previous chapter talked. According to the World Bank (2010), China is now the world's largest

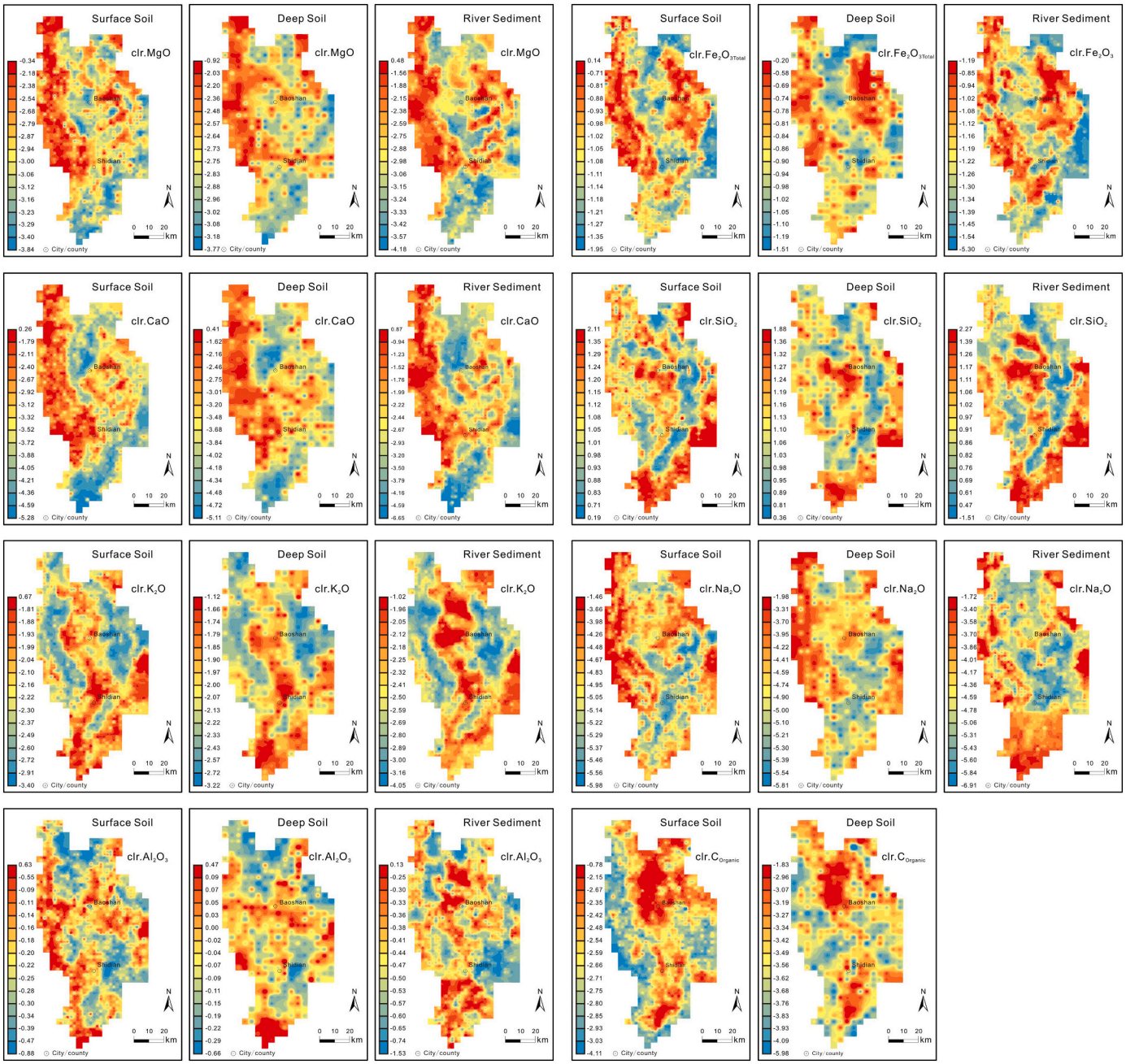

Fig. 4. Major elements geochemical maps of surface soil, deep soil and river sediments in study area.

consumer of chemical fertilizers. The farmland (paddy land) in study area mainly distributed in the flat terrain with lower altitude (Figs. 1 and 2a). The lower altitude and flat topography provided convenient for agricultural fertilization. The fertilizers used in China and study area are mainly inorganic fertilizers (N, P_2O_5, K_2O) and minor organic fertilizer (Fan et al., 2005; Li et al., 2012). The agricultural fertilization may play an important role to those nutrient elements in surface soil of paddy land in the Quaternary areas in the middle area of study area.

PC3: clr. As (−0.67), clr. Hg (−0.76), clr. Sb (−0.74) are strongly associated with high negative loadings from samples adjacent mercury and copper-lead-zinc deposits. The clr. Ga (0.80) and clr. Al_2O_3 (0.78) with high positive loadings are associated with samples taken from clastic rock parent material.

PC4: pH (−0.80), clr. Sr (−0.53), clr. MgO (−0.55), clr. CaO (−0.82) are associated with negative loadings and clr. Br (0.50), clr.I (0.54), clr. Mo (0.54), clr. Se (0.75) are associated with positive loadings. This PC reflects the influence of parent materials such as: samples sourced from basalt rock, Quaternary or carbonate rock parent material show higher pH values and CaO, Sr and MgO concentrations, and lower Br, I, Mo and Se concentrations compares to samples taken from soil derived from other rock type parent material. However, when compared to the land-use map, this PC shows similarity to the spatial distribution of land-use: specifically, the soil data overlying paddy land (pH = 7.37), grassland (pH = 7.15), dry cultivated land (pH = 6.59), garden plot (pH = 6.42) and forest land (pH = 6.04). The higher pH value in paddy land and grass land and lower pH value in forest land, garden plot, and dry cultivated land was also found by other researchers (Han et al., 2007; Islam and Weil, 2000; Barré et al., 2017; Marzaioli et al., 2010; Qin et al., 2016).

PC5: clr. Ag (−0.58), clr. Cd (−0.67), clr. Pb (−0.61), clr. Zn (−0.74) shows strongly negative loadings. This PC is associated with soil samples near the copper-lead-zinc deposits in the study area. The

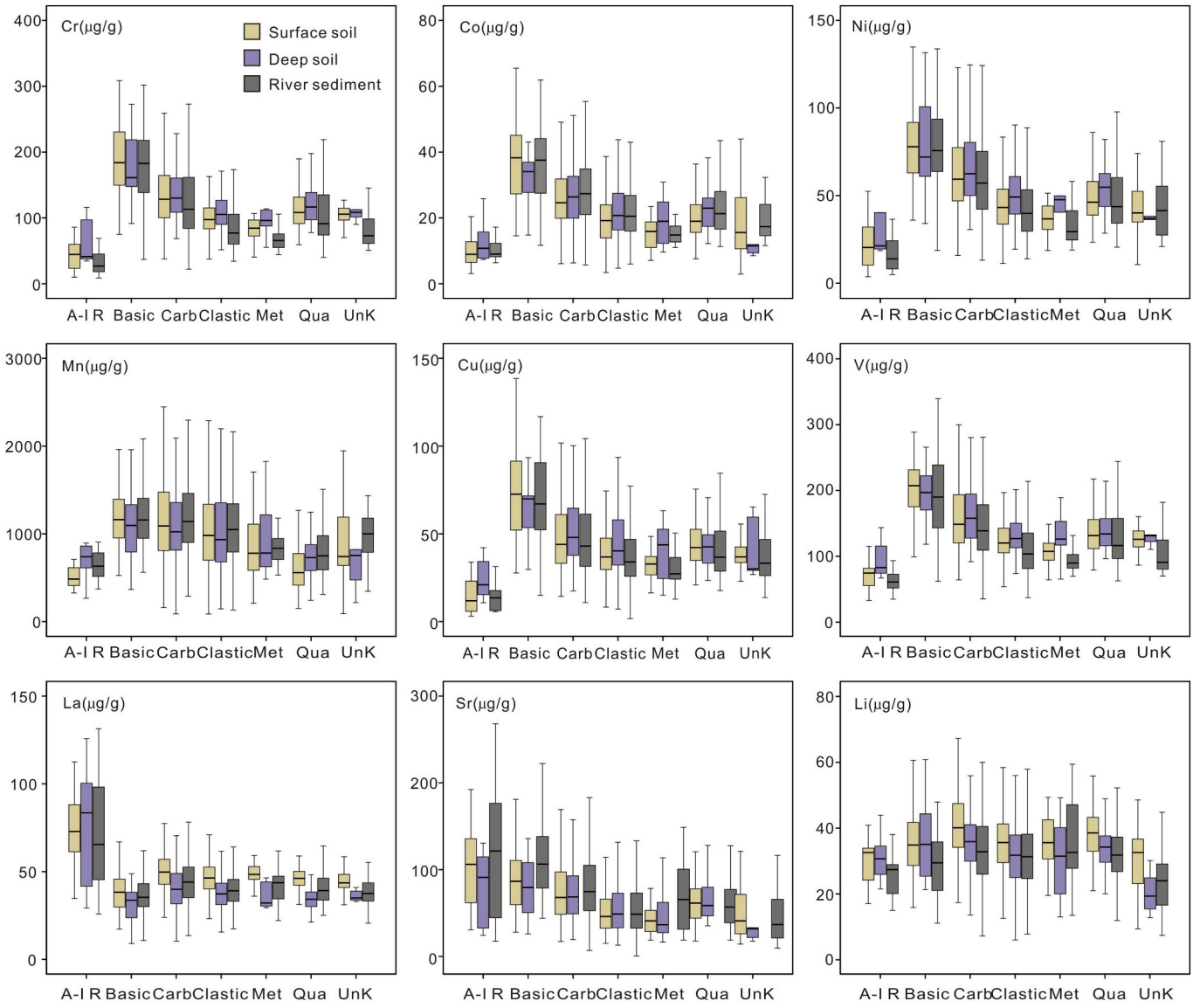

Fig. 5. Box plots of trace elements from soil and river sediments according to rock type groupings.

association of this group of elements is due to Pb coexisting with Zn in the internal growth of a crystal lattice (Mitchell, 1960), and Cd substituting for Zn due to their analogous nature (Alvarezayuso and Garciasanchez, 2003). The association of those elements is also be found in Geochemical Mapping of Agricultural and Grazing Land Soil project (GEMAS) data set (Birke et al., 2017).

3.3.2. Deep soil

Four PCs accounting for 55.4% of the total variance were identified using a scree plot. The results of each PC and the PC geochemical maps are shown in Fig. 9. The following observations were made:

PC1: clr. Co (−0.83), clr. Cr (−0.90), clr. Cu (−0.78), clr. Ni (−0.79), clr. Sc (−0.88), clr. Ti (−0.82), clr. V (−0.93), clr. Fe_2O_{3Total} (−0.90) show high negative loadings. Similar to the surface soil PC1, these elements are associated with samples from soil derived from basic rock parent material. The clr. B (0.53), clr. Rb (0.69), clr. Sn (0.52), clr. Th (0.66), clr. Tl (0.61), clr. K_2O (0.63) have positive loadings. The distribution of these elements is associated with soil sourced from clastic rock parent material in the middle of study area, and acid-intermediate rock parent material in the east.

PC2: clr. SiO_2 (0.61), clr. Al_2O_3 (0.85), clr. K_2O (0.56), clr. Ba (0.58), clr. Be (0.54), clr. Ce (0.57), clr. Ga (0.82), clr.Ge (0.60), clr. Nb (0.57), clr. Rb (0.61), clr. Sn (0.61), clr. Th (0.56) are associated with positive loadings. Those Samples were taken from soil sourced from clastic rock parent material. The clr. Ag (−0.54), clr. As (−0.50), clr. Cd (−0.70), clr. Hg (−0.55), clr. Sb (−0.53), clr. Zn (−0.56) are strongly associated with negative loadings, and are associated with soil mainly near the mercury and copper-lead-zinc deposits.

PC3: clr. Br (−0.63), clr. N (−0.77), clr. S (−0.80), clr. $C_{Orgonic}$ (−0.83), clr. C_{Total} (−0.76) shows high negative loadings, related to soil from the relative higher altitude areas in the middle and northeast of the study area as surface soil described.

PC4: pH (−0.83) and clr.CaO (−0.83) are associated with high negative loadings and clr. Se (0.73) shows positive loading. Similar to the surface soil PC4, these elements mainly controlled by parent material: samples sourced from basalt rock, Quaternary or carbonate rock parent material show higher pH values and CaO concentrations compares to samples taken from soil derived from other rock type parent material; and by a small but important contribution from land-use: the soils from forest land, garden plot and dry cultivated land show lower pH values than grassland and paddy land.

3.3.3. River sediments

Three PCs accounting for 52.3% of the total variance were identified

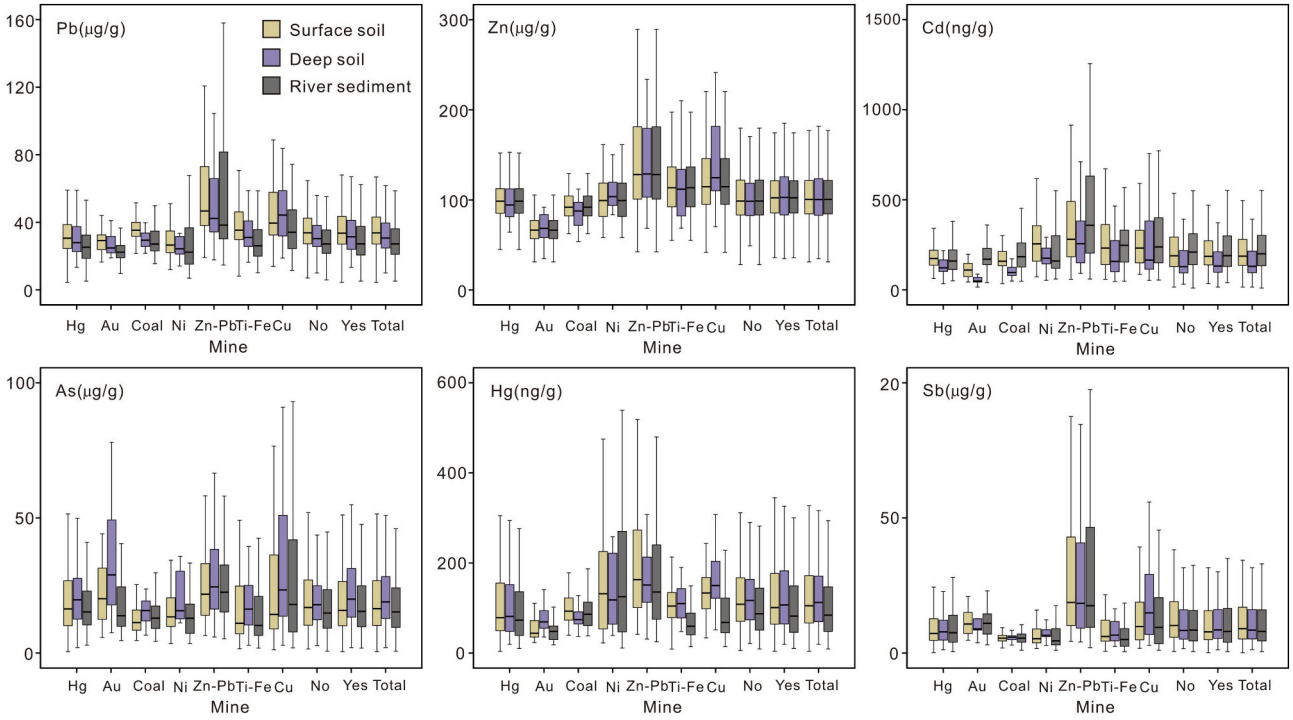

Fig. 6. Box plots of trace elements Pb, Zn, Cd, As, Hg, Sb from soil and river sediments according to the relationship with mineralization.

using a scree plot. The results of each PC and the PC geochemical maps are shown in Fig. 10. The following observations were made:

PC1: clr. MgO (−0.55), clr. Co (−0.88), clr. Cr (−0.93), clr. Cu (−0.79), clr. Ni (−0.86), clr. Ti (−0.62), clr. V (−0.89), clr. Fe_2O_{3Total} (−0.77) shows high negative loadings. The distribution of this group of siderophile elements is associated with river sediments near basic igneous rocks. Conversely, the lithophile elements clr. B (0.61), clr. Ba (0.53), clr. Be (0.58), clr. F (0.58), clr. Th (0.56), clr. U (0.55), clr. W (0.51), clr. Zr (0.54), clr. K_2O (0.73) show positive loadings. The distribution of these elements is associated with river sediments with a clastic rocks source in the middle of the study area, and acid-intermediate rocks in the east of the study area. The distribution of this PC, similar to soil, shows that those elements are proximal to the source they were weathered from.

PC2: clr. Sb (−0.81), clr. As (−0.77), clr. Hg (−0.62), shows high negative loadings associated with river sediments near the mercury and copper-lead-zinc deposits. The clr. Al_2O_3 (0.56) and clr. Nb (0.52) show high positive loadings, and are associated with clastic rocks and acid-intermediate rocks.

PC3: clr. Ag (−0.58), clr. Cd (−0.72), clr. Pb (−0.73), clr. Zn (−0.81) show strong negative loadings associated with samples near the copper-lead-zinc deposits in study area.

In summary, the spatial distribution of these PCs in soil and river sediments reflects the geological and geographical factors of the study area, clearly showing the PC1 in surface soil, deep soil and river sediments are associated with parent materials; PC3 and PC5 in surface soil, PC2 in deep soil, and PC2 and PC3 in river sediment are associated with mineralization; PC2 in surface soil and PC3 in deep soil are mainly associated with altitude, however, agricultural fertilization is also shown to contribute in a minor way to PC2 in surface soil; PC4 in surface soil and deep soil are associated with parent materials, however, land-use is also shown to contribute in a minor way to PC4.

3.4. Anthropogenic impacts

Due to human activities (agricultural fertilizer, urbanization, industries, and mining activities), the fertility of soil can be decreased; especially where the natural background of PTMs is already high due to the nature of the parental material. To assess the anthropogenic impacts, soil contamination assessment was done by calculation of the enrichment factor (EF), which is a widely used proxy (e.g. Akopyan et al., 2018; Barbieri, 2016; Bern et al., 2019; Cevik et al., 2009; Ghrefat et al., 2011; Liénard et al., 2014; Thiombane et al., 2019; Zhang et al., 2014). The deep soil of the NGSLQ program in China shows little effect of human activities. The chemical composition of deep soil is similar to the parent materials, and is used as the soil geochemical background (Cheng et al., 2014b). Aluminum, Ti and Zr are known as immobile element during weathering, they could be used as reference elements to calculate the enrichment factor (Balls et al., 1997; Chen et al., 2007; Horowitz et al., 1988; Reimann and Caritat, 2005; Schropp et al., 1990; Trefry et al., 1985). In this paper, Ti is used as a reference and the following formula was used (Eq. (1)):

$$EF = (C_x/C_{Ti})_{surface}/(C_x/C_{Ti})_{deep} \quad (1)$$

where C_x and C_{Ti} represent the concentration of element x and Ti, respectively.

The numerical results are indicative of different contaminate level. Values of EF ≈ 1 suggest that the trace metal concentration may come entirely from natural weathering processes. However, an EF > 1 indicates that a significant portion of the trace metals was delivered from anthropogenic materials. Barbieri (2016) gave the following interpretation for the enrichment factor: EF < 2, deficient to minimal enrichment; 2 < EF < 5, moderate enrichment; 5 < EF < 20, significant enrichment; 20 < EF < 40, very high enrichment; EF > 40, extremely high enrichment.

For most samples in this study EF ≈ 1, which means the concentration of elements are equal in surface soil and deep soil (background). In some samples, however, EF > 1 is shown in Fig. S3 (Supplementary file). The locations of samples with enrichment of Hg, As, Sb, Cu, Pb, Zn, Cd with the EF > 2 in surface soil are shown in Fig. S4 (Supplementary file), they are mainly located near mine areas. This indicates the contributions of mine activities to the surface soil PTMs (incl. Hg, As, Sb, Cu, Pb, Zn, and Cd). As showed in Fig. S4 (Supplementary file), mercury, copper-lead-zinc, titanium-iron, nickel,

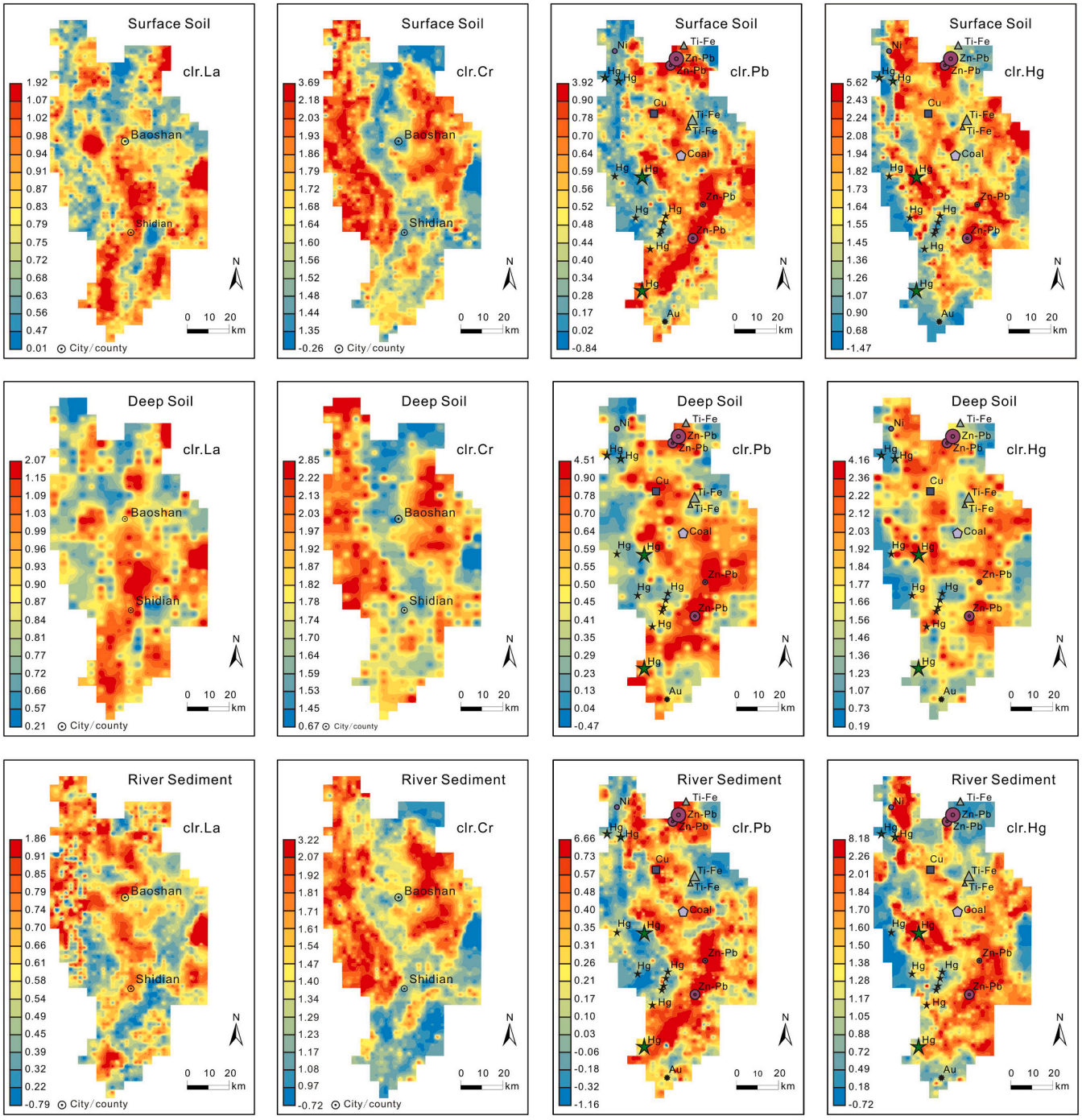

Fig. 7. Geochemical maps of trace elements in soil and river sediments. Mineralization occurrences plotted for comparison in Pb and Hg geochemical map.

coal and gold mineralization and deposits are widely distributed in the study area and they have been massively mined during latest 20–30 years. For Pb, Zn and Cu, the enrichment in surface soil mainly occurs within 2 km of copper-lead-zinc deposits. For Cd, the enrichment in surface soil is widely distributed in the study area, and it is highly coincidence with the distribution of PC5 in surface soil. For Hg, As and Sb the enrichment in surface soil is mainly near mercury and copper-lead-zinc mineralization and deposits, the distribution of the enrichment is >10 km far from the mine center location. Those mercury and copper-lead-zinc deposits including historic mine already finish mining and mine still ongoing. Administrators and researches are critically needed to strengthen mining regulations to protect the nearby farmland, though no crops with those PTMs exceed national standards have been reported in study areas for now.

The urbanization (factories, paint, vehicle exhausts, etc.) also the main factor leading to PTMs pollution in surface soil in the world wide and China (Cicchella et al., 2016; Chen et al., 2005; Hamzeh et al., 2011; Poňavič et al., 2018; Rate, 2018; Teutsch et al., 2001; Luo et al., 2012; Goldhaber et al., 2009). Prior to the phasing out of leaded petrol, lead was a significant component of traffic derived soil contamination in urban soils (Callender and Rice, 2000). Lead, Cu, and Zn are three of the most common heavy metals released from automobiles, accounting for at least 90% of total metals in road runoff (Thomas, 1995). While, the major economic industries are mining and agriculture in the Baoshan area. The Baoshan area is still a relatively underdeveloped and remote area in China, even though it is developed since the last

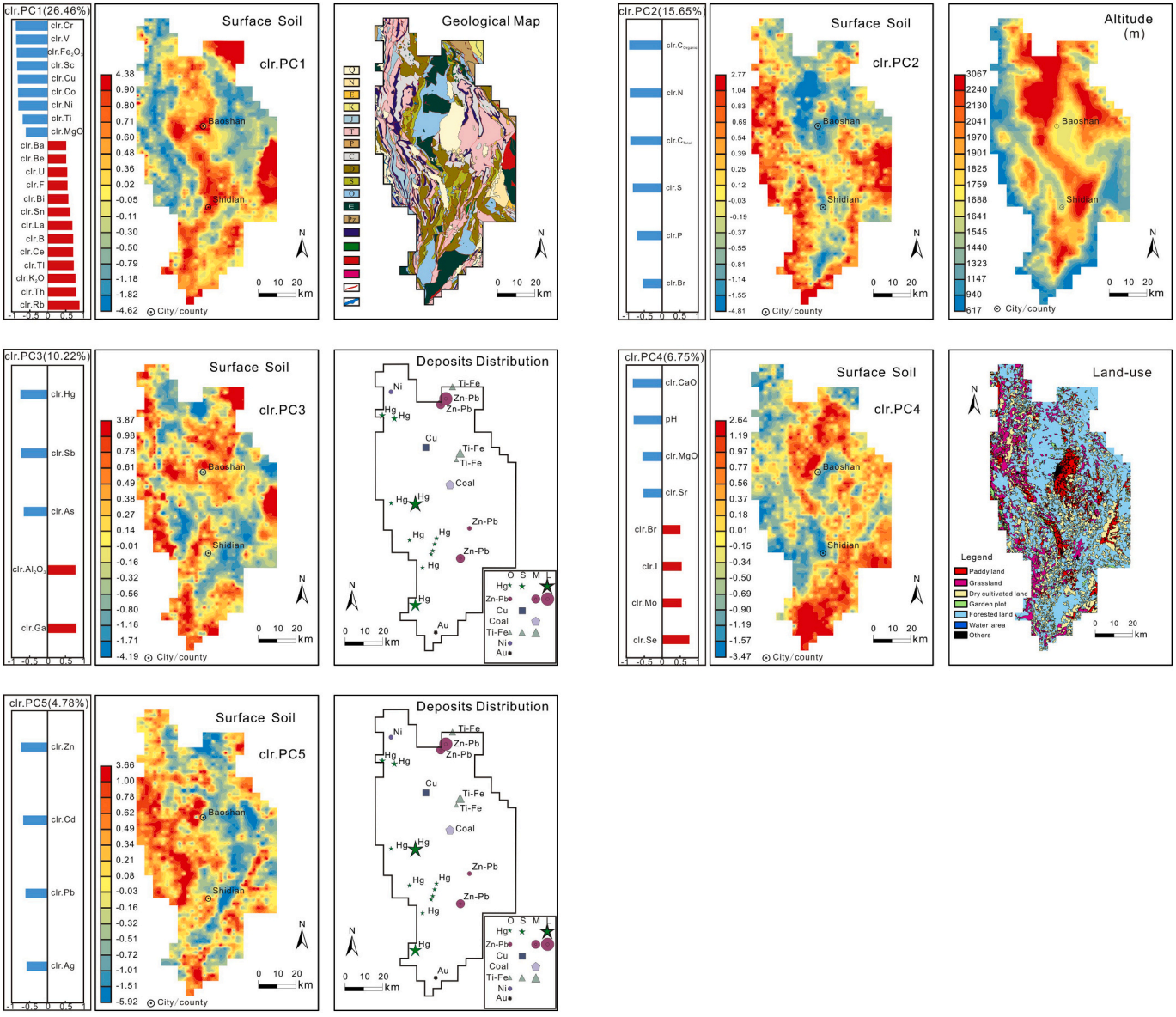

Fig. 8. Spatial distribution of PCs of surface soil. Geological, mineralization, altitude and land-use maps are presented for comparison.

20–30 years. Except for Baoshan city center and Shidian county center (Fig. 2b), all the rest are rural areas. As described in the Supplementary file the surface soil within 100 m from a major road or a railway were avoided during sampling. So, urbanization may not the considerable factor in the PTMs pollution in surface soil in this study.

4. Conclusion

The results of this study provide an insight into the element concentration and patterns of surface soil, deep soil and river sediments, and the factors that influence their distribution in Baoshan area, Yunnan province, China.

The statistical summary for soil and river sediments in Baoshan area shows that the elements As, B, (Br), Co, Cr, Cu, Hg, (I), Mn, (N), Ni, Sb, (Sc), (Se), V, Fe_2O_{3Total} and ($C_{Orgonic}$) concentrations are enriched in the Baoshan area compared to the CGB and RGNR data set. The elements Sr and Na_2O are depleted compared to the CGB and RGNR data set.

By combining single element geochemical, geological, mineralization, altitude, temperature and land-use maps, the median value of differing rock types and the relationship to mineralization, the factors influencing elements in soil and river sediments in the study area were investigated. The distribution of most elements are controlled by the geological parent material: Co, Cr, Cu, Ni, Sc, Ti, V, Fe_2O_{3Total}, MgO are controlled by basic rock sources; As, Hg, Sb, (Ag), Cd, Pb, Zn are controlled by mineralization; other elements are largely controlled by clastic rocks and acid-intermediate rocks; Ca, Mg, Sr and pH are mainly controlled by basalt rock, carbonate rock and Quaternary sources. However, land-use also has a minor contribution to the distribution of Ca, Mg, Sr and pH. While C_{Total}, Br, N, (P), S, and $C_{Orgonic}$ in soil was controlled by geomorphic (altitude/temperature) changes, but agricultural fertilization in Quaternary area has caused those elements enrichment in surface soil.

Finally, anthropogenic factors (mining activities) have also been recognized in the soil data set and are responsible for the surface soil contamination by PTMs (incl. Hg, As, Sb, Cu, Pb, Zn, Cd) near mining areas.

CRediT authorship contribution statement

Li Zhang: Conceptualization, Writing - original draft. **Jennifer McKinley:** Writing - review & editing. **Mark Cooper:** Writing - review & editing. **Min Peng:** Project administration,

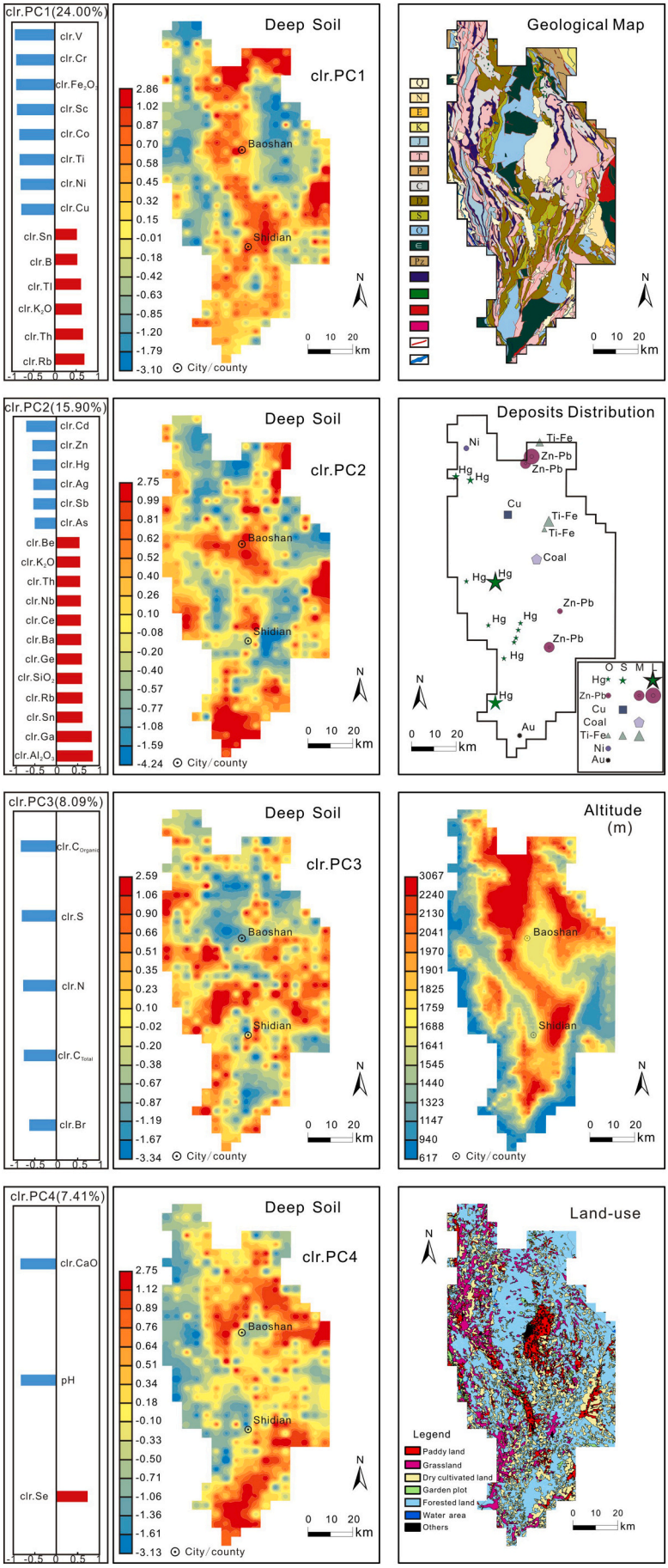

Fig. 9. Spatial distribution of PCs of deep soil. Geological, mineralization, altitude and land-use maps are presented for comparison.

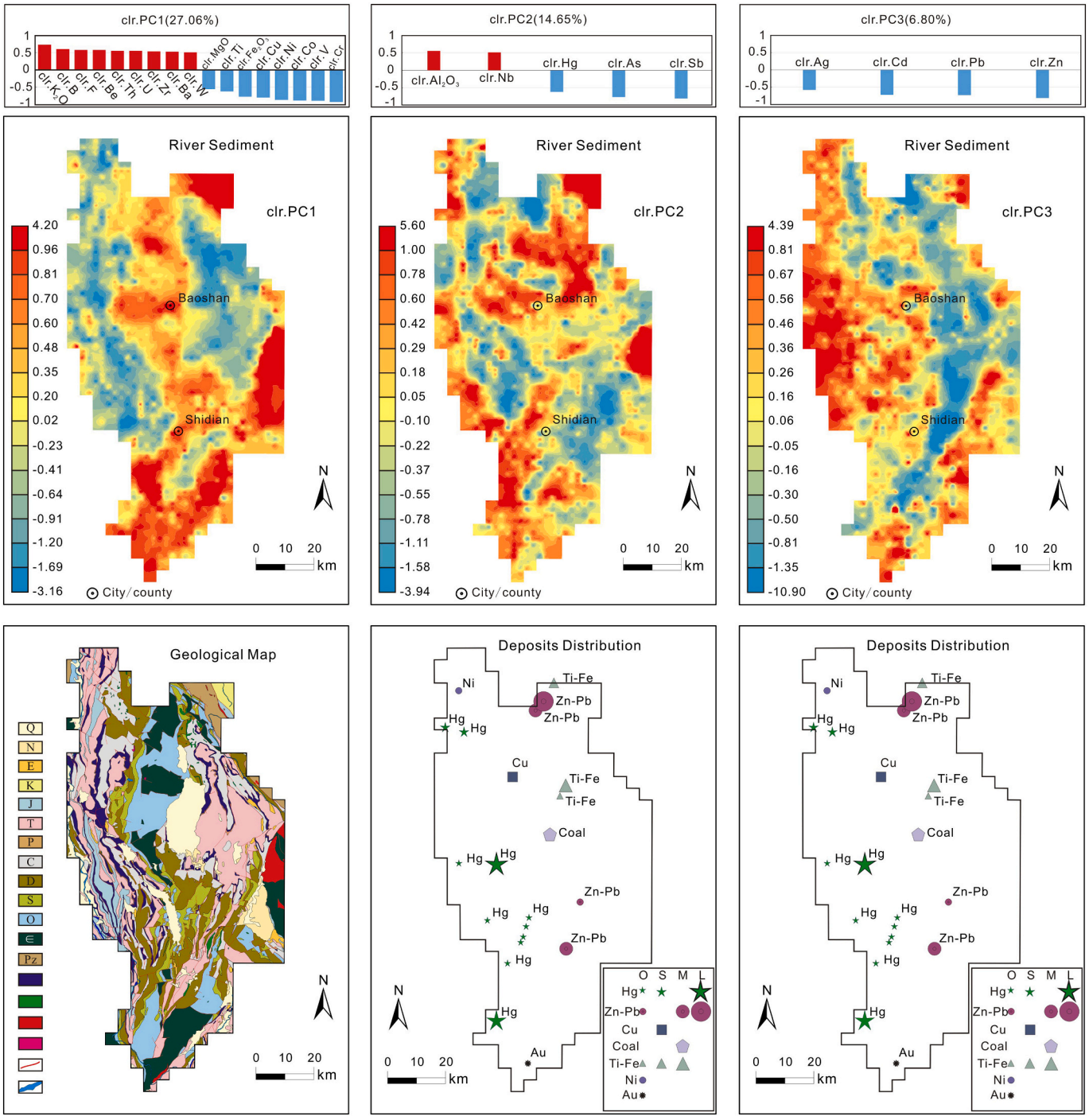

Fig. 10. Spatial distribution of PCs of river sediments. Geological and mineralization maps are presented for comparison.

Conceptualization. **Qiaolin Wang**: Project administration. **Yuntao Song**: Project administration. **Hangxin Cheng**: Project administration, Conceptualization.

Declaration of competing interest

The authors declare that they have no known competing financial interests or personal relationships that could have appeared to influence the work reported in this paper.

Acknowledgements

The authors would like to thank the funding provided by China Geological Survey (DD20160313) and Ministry of Finance of China Foundation (121201108000168530) and China Scholarship Council (CSC201868110267). Acknowledgement for the data support from "National Earth System Science Data Sharing Infrastructure, National Science & Technology Infrastructure of China (http://www.geodata.cn)". We would like to appreciate to all of the participants from Division of Geochemical Survey Methodology, IGGE for the field work. Thanks to Dr. Jian Zhou from International Centre on Global-Scale Geochemistry, UNESCO and Dr. Bingli Liu from Chengdu University of Technology, China for the useful suggestions to this paper. Finally, the

authors would like to express our sincere thanks to the editors and reviewers for their critical and constructive comments and suggestions.

Appendix A. Supplementary data

Supplementary data to this article can be found online at https://doi.org/10.1016/j.gexplo.2020.106557.

References

(The) World Bank, 2010. World Development Indicators 2010. The World Bank, Washington,DC available at. www.worldbank.org.

Addo, M.A., Darko, E.O., Gordon, C., Nyarko, B.J.B., Gbadago, J.K., Nyarko, E., Affum, H.A., Botwe, B.O., 2012. Evaluation of heavy metals contamination of soil and vegetation in the vicinity of a cement factory in the Volta Region, Ghana. International Journal of Science & Technology 2, 40–50.

Aitchison, J., 1981. A new approach to null correlations of proportions. J. Int. Assoc. Math. Geol. 13, 175–189.

Aitchison, J., 1982. The statistical analysis of compositional data (with discussion). J. R. Stat. Soc. Ser. B Stat Methodol. 44 (2), 139–177.

Aitchison, J., 1986. The statistical analysis of compositional data. In: Monographs on Statistics and Applied Probability. Chapman & Hall Ltd., London (UK) (Reprinted in 2003 with additional material by The Blackburn Press), London (UK) (416 p) (1986).

Akopyan, K., Petrosyan, V., Grigoryan, R., Melkom Melkomian, D., 2018. Assessment of residential soil contamination with arsenic and lead in mining and smelting towns of northern Armenia. J. Geochem. Explor. 184, 97–109.

Albanese, S., De Vivo, B., Lima, A., Cicchella, D., 2007. Geochemical background and baseline values of toxic elements in stream sediments of Campania region (Italy). J. Geochem. Explor. 93, 21–34.

Alvarezayuso, E., Garciasanchez, A., 2003. Sepiolite as a feasible soil additive for the immobilization of cadmium and zinc. Sci. Total Environ. 305, 1–12.

Antibachi, D., Kelepertzis, E., Kelepertsis, A., 2012. Heavy metals in agricultural soils of the Mouriki-Thiva Area (Central Greece) and environmental impact implications. Soil Sediment Contam. Int. J. 21, 434–450.

Balls, P.W., Hull, S., Miller, B.S., Pirie, J.M., Proctor, W., 1997. Trace metal in Scottish estuarine and coastal sediments. Mar. Pollut. Bull. 34, 42–50.

Barbieri, M., 2016. The importance of enrichment factor (EF) and geoaccumulation index (Igeo) to evaluate the soil contamination. J. Geol. Geophys. 5.

Barré, P., Durand, H., Chenu, C., Meunier, P., Montagne, D., Castel, G., Billiou, D., Soucémarianadin, L., Cécillon, L., 2017. Geological control of soil organic carbon and nitrogen stocks at the landscape scale. Geoderma 285, 50–56.

Barsby, A., McKinley, J.M., Ofterdinger, U., Young, M., Cave, M.R., Wragg, J., 2012. Bioaccessibility of trace elements in soils in Northern Ireland. Sci. Total Environ. 433, 398–417.

Becquer, T., Quantin, C., Rotte-Capet, S., Ghanbaja, J., Mustin, C., Herbillon, A.J., 2006. Sources of trace metals in ferralsols in New Caledonia. Eur. J. Soil Sci. 57, 200–213.

Bern, C.R., Walton-Day, K., Naftz, D.L., 2019. Improved enrichment factor calculations through principal component analysis: examples from soils near breccia pipe uranium mines, Arizona, USA. Environ. Pollut. 248, 90–100.

Birke, M., Reimann, C., Rauch, U., Ladenberger, A., Demetriades, A., Jähne-Klingberg, F., Oorts, K., Gosar, M., Dinelli, E., Halamić, J., 2017. GEMAS: cadmium distribution and its sources in agricultural and grazing land soil of Europe-original data versus clr-transformed data. J. Geochem. Explor. 173, 13–30.

Bompoti, N., Chrysochoou, M., Dermatas, D., 2015. Geochemical characterization of Greek ophiolitic environments using statistical analysis. Environmental Processes 2, 5–21.

Bonifacio, E., Falsone, G., Piazza, S., 2010. Linking Ni and Cr concentrations to soil mineralogy: does it help to assess metal contamination when the natural background is high? J. Soils Sediments 10, 1475–1486.

Boogaart, K., Tolosana-Delgado, R., 2013. Analyzing Compositional Data With R. pp. 73–93.

Cabral Pinto, M.M.S., Silva, M.M.V.G., Ferreira da Silva, E.A., Dinis, P.A., Rocha, F., 2017. Transfer processes of potentially toxic elements (PTE) from rocks to soils and the origin of PTE in soils: a case study on the island of Santiago (Cape Verde). J. Geochem. Explor. 183, 140–151.

Callender, E., Rice, K.C., 2000. The urban environmental gradient: anthropogenic influences on the spatial and temporal distributions of lead and zinc in sediments. Environ. Sci. Technol. 34, 232–238.

Cevik, F., Goksu, M.Z., Derici, O.B., Findik, O., 2009. An assessment of metal pollution in surface sediments of Seyhan dam by using enrichment factor, geoaccumulation index and statistical analyses. Environ. Monit. Assess. 152, 309–317.

CGS, 2005. Specification for Multi-purpose Regional Geochemical Survey (DD2005-01). In: China Geological Survey, Beijing. (In Chinese).

CGS, 2014. Specification for Multi-purpose Regional Geochemical Survey (DD/T 0258-2014). In: China Geological Survey, Beijing. (In Chinese).

Chayes, F., 1960. On correlation between variables of constant sum. J. Geophys. Res. 65 (12), 4185–4193.

Chen, J., Tan, M., Li, Y., Zhang, Y., Lu, W., Tong, Y., Lu, W., Tong, Y., Zhang, G., Li, Y., 2005. A lead isotope record of shanghai atmospheric lead emissions in total suspended particles during the period of phasing out of leaded gasoline. Atmos. Environ. 39 (7), 1245–1253.

Chen, C.W., Kao, C.M., Chen, C.F., Dong, C.D., 2007. Distribution and accumulation of heavy metals in the sediments of Kaohsiung Harbor, Taiwan. Chemosphere 66 (8), 1431–1440.

Cheng, X.M., 2016. Geochemical Behavior and Risk Analysis for Heavy Elements in Soil Profiles With Different Parent Material, Yunnan Province, China. (in Chinese with English abstract).

Cheng, H.X., Li, M., Xie, X.J., Yang, Z.F., Li, C., 2014a. Exploring China: environment and resources. Journal of Geochemical Exploration: Journal of the Association of Exploration Geochemists 1–216.

Cheng, H.X., Li, K., Li, M., Yang, K., Liu, F., Cheng, X.M., 2014b. Geochemical background and baseline value of chemical elements in urban soil in China. Earth Science Frontiers 21 (3), 265–306 (in Chinese with English abstract).

Chiu, Y.P., Li, D.W., Shiau, Y.C., 2016. Study on heavy metal characteristics of soil in phosphorus tail. J. Residuals Sci. Technol. 13.

Cicchella, D., De, V.B., Lima, A., Albanese, S., Mc, G.R.A.R., Parrish, R.R., 2008. Heavy metal pollution and Pb isotopes in urban soils of Napoli, Italy. Geochemistry Exploration Environment Analysis 8, 103–112.

Cicchella, D., Hoogewerff, J., Albanese, S., Adamo, P., Lima, A., Taiani, M.V.E., Benedetto De Vivo, B., 2016. Distribution of toxic elements and transfer from the environment to humans traced by using lead isotopes. A case of study in the Sarno River Basin, South Italy. Environ. Geochem. Health 38 (2), 619–637.

Cox, S.F., Rollinson, G., McKinley, J.M., 2017. Mineralogical characterisation to improve understanding of oral bioaccessibility of Cr and Ni in basaltic soils in Northern Ireland. J. Geochem. Explor. 183, 166–177.

Darnley, A., Garrett, R.G., 1990. International geochemical mapping special issue. J. Geochem. Explor. 39.

Darnley, A.G., Bjiirklund, A., Belviken, B., Gustavsson, N., Koval, P.V., Plant, J.A., Steenfelt, A., Tauchid, M., Xuejing, X., 1995. A Global Geochemical Database for Environmental and Resource Management: Recommendations for International Geochemical Mapping: Final Report of IGCP Project 259. UNESCO Publishing.

Dokuchaev, V.V., 1967. Russian chernozem. In: Selected Works of V. V. Dokuchaev, Moscow, 1948. 1. Israel Program for Scientific Translations Ltd. (for USDA-NSF), Publ. by S. Monson, Jerusalem (Transl. into English by N. Kaner), pp. 14–419.

Dong, M., Dong, G., Mo, X., Santosh, M., Zhu, D., Yu, J., Nie, F., Hu, Z., 2013. Geochemistry, zircon U–Pb geochronology and Hf isotopes of granites in the Baoshan Block, Western Yunnan: implications for Early Paleozoic evolution along the Gondwana margin. Lithos 179, 36–47.

Egozcue, J.J., Pawlowsky-Glahn, V., Mateu-Figueras, G., Barceló-Vidal, C., 2003. Isometric logratio transformations for compositional data analysis. Math. Geol. 35, 279–300.

Fan, M., Zheng, Y., Li, S., Mao, K., Yin, S., Zhou, H., 2005. Nutrient cycling and balance of agro-ecosystem in Baoshan, Yunnan Province. Journal of Yunnan Agricultural University 20 (3), 415–418 (in Chinese with English abstract).

Gałuszka, A., 2007. Different approaches in using and understanding the term “geochemical background” - practical implications for environmental studies. Polish J. Environ. Stud. 16, 389–395.

Ghrefat, H.A., Abu-Rukah, Y., Rosen, M.A., 2011. Application of geoaccumulation index and enrichment factor for assessing metal contamination in the sediments of Kafrain Dam, Jordan. Environ. Monit. Assess. 178, 95–109.

Goldhaber, M.B., Morrison, J.M., Holloway, J.M., Wanty, R.B., Helsel, D.R., Smith, D.B., 2009. A regional soil and sediment geochemical study in northern California. Appl. Geochem. 24, 1482–1499.

Hamzeh, M.A., Aftabi, A., Mirzaee, M., 2011. Assessing geochemical influence of traffic and other vehicle-related activities on heavy metal contamination in urban soils of Kerman city, using a GIS-based approach. Environ. Geochem. Health 33, 577–594.

Han, S.C., Pu, L.J., Chen, F., Zhang, C.Y., Zhang, J., Peng, B.Z., 2007. Responses of soil properties to change in land-use in a typical area of the Yangtze river delta - a case study of Xishan city, Jiangsu province, China. Acta Pedol. Sin. 44 (4) (612-319. in Chinese with English abstract).

Horowitz, A.J., Elrick, K., Callender, E., 1988. The effect of mining on the sediment-trace element geochemistry of cores from the Cheyenne River arm of Lake Oahe, South Dakota, USA. Chem. Geol. 67, 17–33.

Islam, K.R., Weil, R.R., 2000. Land use effects on soil quality in a tropical forest ecosystem of Bangladesh. Agric. Ecosyst. Environ. 79, 9–16.

Jenny, H., 1941. Factors of Soil Formation: A System of Quantitative Pedology. McGraw-Hill, New York, pp. 281.

Kelepertzis, E., Galanos, E., Mitsis, I., 2013. Origin, mineral speciation and geochemical baseline mapping of Ni and Cr in agricultural topsoils of Thiva Valley (central Greece). J. Geochem. Explor. 125, 56–68.

Leifeld, J., Bassin, S., Fuhrer, J., 2005. Carbon stocks in Swiss agricultural soils predicted by land-use, soil characteristics, and altitude. Agric. Ecosyst. Environ. 105, 255–266.

Li, X.H., Cheng, H.X., Zhao, C.D., Xu, X.B., 2010. Mercury contamination in the topsoil and subsoil of urban areas of Beijing, China. Bull. Environ. Contam. Toxicol. 85, 224–228.

Li, Y., Fredrich, Kahrl., Pan, J., Roland-Holst, D., Su, Yufang., Wilkes, A., Xu, J., 2012. Fertilizer use patterns in Yunnan Province, China: implications for agricultural and environmental policy. Agric. Syst. 110, 78–89.

Li, M., Xi, X., Xiao, G., Cheng, H., Yang, Z., Zhou, G., Ye, J., Li, Z., 2014a. National multi-purpose regional geochemical survey in China. J. Geochem. Explor. 139, 21–30.

Li, Z., Ma, Z., van der Kuijp, T.J., Yuan, Z., Huang, L., 2014b. A review of soil heavy metal pollution from mines in China: pollution and health risk assessment. Sci. Total Environ. 468–469, 843–853.

Li, D., Chen, Y., Hou, K., Lu, Z., Cui, D., 2015. Detrital zircon record of Paleozoic and Mesozoic meta-sedimentary strata in the eastern part of the Baoshan block: implications of their provenance and the tectonic evolution of the southeastern margin of the Tibetan plateau. Lithos 227, 194–204.

Liénard, A., Brostaux, Y., Colinet, G., 2014. Soil contamination near a former Zn–Pb ore-treatment plant: evaluation of deterministic factors and spatial structures at the

landscape scale. J. Geochem. Explor. 147, 107–116.
Luo, X.S., Yu, S., Zhu, Y.G., Li, X.D., 2012. Trace metal contamination in urban soils of China. Sci. Total Environ. 421–422, 17–30.
Marzaioli, R., D'Ascoli, R., De Pascale, R.A., Rutigliano, F.A., 2010. Soil quality in a Mediterranean area of Southern Italy as related to different land use types. Appl. Soil Ecol. 44, 205–212.
McGrath, D., Tunney, H., 2010. Accumulation of cadmium, fluorine, magnesium, and zinc in soil after application of phosphate fertilizer for 31 years in a grazing trial. J. Plant Nutr. Soil Sci. 173, 548–553.
Mckinley, J.M., Hron, K., Grunsky, E.C., Reimann, C., Caritat, P.D., Filzmoser, P., Boogaart, K.G.V.D., Tolosana-Delgado, R., 2016. The single component geochemical map: fact or fiction. J. Geochem. Explor. 162, 16–28.
Mitchell, R.L., 1960. Trace element problems in Scottish soils. Proc. Nutr. Soc. 19, 148–153.
Pawlowsky-Glahn, V., Buccianti, A., 2011. Compositional Data Analysis: Theory and Applications. John Wiley & Sons (378 p).
Pawlowsky-Glahn, V., Egozcue, J.J., 2001. Geometric approach to statistical analysis on the simplex. Stoch. Env. Res. Risk A. 15, 384–398.
Plant, J., Smith, D., Smith, B., Williams, L., 2001. Environmental geochemistry at the global scale. Appl. Geochem. 16, 1291–1308.
Poňavič, M., Wittlingerová, Z., Čoupek, P., Jan, B., 2018. Soil geochemical mapping of the central part of Prague, Czech Republic. J. Geochem. Explor. 187, 118–130.
Qin, C., He, B.H., Jiang, X.J., 2016. Soil nutrient characteristics of different land-use types in the Tree Gorges Reservoir. Acta Pratacul. Sin. 25 (9), 10–19 (in Chinese with English abstract).
Qu, C., Sun, Y., Albanese, S., Lima, A., Sun, W., Di Bonito, M., Qi, S., De Vivo, B., 2017. Organochlorine pesticides in sediments from Gulfs of Naples and Salerno, Southern Italy. J. Geochem. Explor. 195, 87–96.
Qu, C., Albanese, S., Lima, A., Hope, D., Pond, P., Fortelli, A., Romano, N., Cerino, R., Pizzolante, A., De Vivo, B., 2019. The occurrence of OCPs, PCBs, and PAHs in the soil, air, and bulk deposition of the Naples metropolitan area, southern Italy: implications for sources and environmental processes. Environ. Int. 124, 89–97.
Rate, A.W., 2018. Multielement geochemistry identifies the spatial pattern of soil and sediment contamination in an urban parkland, Western Australia. Sci. Total Environ. 627, 1106–1120.
Reimann, C., Caritat, P., 2005. Distinguishing between natural and anthropogenic sources for elements in the environment: regional geochemical surveys versus enrichment factors. Sci. Total Environ. 337, 91–107.
Reimann, C., Caritat, P., 2017. Establishing geochemical background variation and threshold values for 59 elements in Australian surface soil. Sci. Total Environ. 578, 633–648.
Sahoo, P.K., Dall'Agnol, R., Salomão, G.N., Junior, J.D.S.F., Silva, M.S., e Souza Filho, P.W.M., Powell, M.A., Angélica, R.S., Pontes, P.R., da Costa, M.F., Siqueira, J.O., 2019a. High resolution hydrogeochemical survey and estimation of baseline concentrations of trace elements in surface water of the Itacaiúnas River Basin, southeastern Amazonia: implication for environmental studies. J. Geochem. Explor. 205, 106321.
Sahoo, P.K., Guimarães, J.T.F., Souza-Filho, P.W.M., Powell, M.A., da Silva, M.S., Moraes, A.M., Alves, R., Leite, A.S., Júnior, W.N., Rodrigues, T.M., Costa, V.E., Dall'Agnol, E., 2019b. Statistical analysis of lake sediment geochemical data for understanding surface geological factors and processes: an example from Amazonian upland lakes, Brazil. Catena 175, 47–62.
Sahoo, P.K., Dall'Agnol, R., Salomão, G.N., Junior, J.D.S.F., da Silva, M.S., Martins, G.C., e Souza Filho, P.W.M., Powell, M.A., Maurity, C.W., Angelica, R.S., da Costa, M.F., Siqueira, J.O., 2020. Source and background threshold values of potentially toxic elements in soils by multivariate statistics and GIS-based mapping: a high density sampling survey in the Parauapebas basin, Brazilian Amazon. Environ. Geochem. Health 42 (1), 255–282.
Salomão, G.N., Figueiredo, M.A., Dall'Agnol, R., Sahoo, P.K., de Medeiros Filho, C.A., da Costa, M.F., Angélica, R.S., 2019. Geochemical mapping and background concentrations of iron and potentially toxic elements in active stream sediments from Carajás, Brazil–implication for risk assessment. J. S. Am. Earth Sci. 92, 151–166.
Schropp, S.J., Lewis, F.G., Windom, H.L., Ryan, J.D., Calder, F.D., Burney, L.C., 1990. Interpretation of metal concentrations is estuarine sediments of Florida using aluminum as a reference element. Estuaries 13, 227–235.
Shi, C.Y., Liang, M., Feng, B., 2016. Average background values of 39 chemical elements in stream sediments of China. Earth Sci. 41 (2), 234–251 (in Chinese with English abstract).
Tashakor, M., Wan Zuhairi, Y., Mohamad, H., Ghani, A., 2014. Geochemical characteristics of serpentinite soils from Malaysia. Malaysian Journal of Soil Science 18, 35–49.
Teutsch, N., Erel, Y., Halicz, L., Banin, A., 2001. Distribution of natural and anthropogenic lead in mediterranean soils. Geochim. Cosmochim. Acta 65 (17), 2853–2864.
Thio-Henestrosa, S., Martin-Fernandez, J.A., 2006. Detailed guide to CoDaPack: a freeware compositional software. Geological Society London Special Publications 264, 101–118.
Thiombane, M., Di Bonito, M., Albanese, S., Zuzolo, D., Lima, A., De Vivo, B., 2019. Geogenic versus anthropogenic behaviour and geochemical footprint of Al, Na, K and P in the Campania region (Southern Italy) soils through compositional data analysis and enrichment factor. Geoderma 335, 12–26.
Thomas, V., 1995. The elimination of lead in gasoline. Annual Review Energy Environment 20 (2), 301–324.
Tolosana-Delgado, R., McKinley, J., 2016. Exploring the joint compositional variability of major components and trace elements in the Tellus soil geochemistry survey (Northern Ireland). Appl. Geochem. 75, 263–276.
Trefry, J.H., Metz, S., Trocine, R.P., 1985. A decline in lead transport by the Mississippi River. Science 230, 439–441.
Wang, Y., Zhang, A., Fan, W., Peng, T., Zhang, F., Zhang, Y., Bi, X., 2010. Petrogenesis of late Triassic post-collisional basaltic rocks of the Lancangjiang tectonic zone, southwest China, and tectonic implications for the evolution of the eastern Paleotethys: geochronological and geochemical constraints. Lithos 120, 529–546.
Wang, Y., Xing, X., Cawood, P.A., Lai, S., Xia, X., Fan, W., Liu, H., Zhang, F., 2013. Petrogenesis of early Paleozoic peraluminous granite in the Sibumasu Block of SW Yunnan and diachronous accretionary orogenesis along the northern margin of Gondwana. Lithos 182, 67–85.
Wang, X., Liu, X., Han, Z., Zhou, J., Xu, S., Zhang, Q., Chen, H., Bo, W., Xia, X., 2015. Concentration and distribution of mercury in drainage catchment sediment and alluvial soil of China. J. Geochem. Explor. 154, 32–48.
Wang, X.Q., Zhou, J., Xu, S.F., Chi, Q.H., Nie, L.S., Zhang, B.M., YAO, W.S., Wang, Wei., Liu, H.L., Liu, D.S., Han, Z.X., Liu, Q.Q., 2016. China soil geochemical baselines networks: data characteristics. Geol. China 43 (5), 1469–1480 (in Chinese with English abstract).
Wiesmeier, M., Hübner, R., Barthold, F., Spörlein, P., Geuß, U., Hangen, E., Reischl, A., Schilling, B., von Lützow, M., Kögel-Knabner, I., 2013. Amount, distribution and driving factors of soil organic carbon and nitrogen in cropland and grassland soils of southeast Germany (Bavaria). Agric. Ecosyst. Environ. 176, 39–52.
Xie, X., Cheng, H., 2014. Sixty years of exploration geochemistry in China. J. Geochem. Explor. 139, 4–8.
Xie, X., Wang, X., Zhang, Q., Zhou, G., Cheng, H., Liu, D., Cheng, Z., Xu, S., 2008. Multiscale geochemical mapping in China. Geochemistry: Exploration, Environment, Analysis 8, 333–341.
Yuan, G.L., Sun, T.H., Han, P., Li, J., 2013. Environmental geochemical mapping and multivariate geostatistical analysis of heavy metals in topsoils of a closed steel smelter: Capital Iron & Steel Factory, Beijing, China. J. Geochem. Explor. 130, 15–21.
Zhang, X.P., Wei, D., Yang, X.M., 2002. The background concentrations of 13 soil trace elements and their relationships to parent materials and vegetation in Xizang (Tibet), China. J. Asian Earth Sci. 21, 167–174.
Zhang, H., Luo, Y., Makino, T., Wu, L., Nanzyo, M., 2013. The heavy metal partition in size-fractions of the fine particles in agricultural soils contaminated by waste water and smelter dust. J. Hazard. Mater. 248–249, 303–312.
Zhang, H., Chen, J., Li, Z., Yang, G., Li, D., 2014. Anthropogenic mercury enrichment factors and contributions in soils of Guangdong Province, South China. J. Geochem. Explor. 144, 312–319.
Zheng, K.L., Ye, J.Y., Jiang, B.L., 2005. Selected Analytical Methods of 57 Elements for Multi-purpose Geochemical Survey. Geological Publishing House, Beijing (in Chinese).